

A Hitchhiker’s Guide to Temporal Complexity for Resting State fMRI Analysis

Isabel Si-En Wilson^a, Andre Reza Zamani^b, Alexander Mark Weber^{a,c,*}

^a*BC Children’s Hospital Research Institute, The University of British Columbia, Vancouver, BC, Canada,*

^b*Department of Psychology, The University of British Columbia, Vancouver, BC, Canada,*

^c*Department of Pediatrics, The University of British Columbia, Vancouver, BC, Canada,*

Abstract

For decades, fMRI analysis has predominantly focused on linear relationships, such as simple signal magnitude changes and pair-wise functional connectivity. Recent evidence suggests that failing to account for the brain’s non-linear, dynamic organization may lead to incomplete inferences about neural processes. More recently, cognitive and clinical neuroimaging have begun to draw on tools from complexity science to characterize the nonlinear dynamics of the brain. Temporal complexity metrics reflect a range of approaches to complexity in time series, including describing the system’s regularity and irregularity, predictability and unpredictability, information compressibility, long-term memory, and fractal patterns. In functional magnetic resonance imaging (fMRI), applications of temporal complexity are scattered across siloed literatures with varying clarity, which limits accessibility and therefore popularity. This review aims to bridge this gap by communicating the basics of temporal complexity to fMRI scientists. We offer a comprehensive guide to temporal complexity in fMRI, including an overview of fMRI temporal complexity metrics—Shannon entropy, variations of (multi-scale) sample entropy, Lempel-Ziv complexity, avalanche measures, and Hurst—followed by a comprehensive review of extant applications in fMRI.

Keywords: temporal complexity, complexity, entropy, sample entropy, hurst exponent, fractal dimension, fractal, functional magnetic resonance imaging, resting-state, nonlinear dynamics, neuroscience, brain, blood-oxygen level dependence, predictability, irregularity, long-range temporal correlations, long-term memory, scale-invariance, power-law

*Corresponding author

Email addresses: isabelsienw@gmail.com (Isabel Si-En Wilson), azamani@psych.ubc.ca (Andre Reza Zamani), a.weber@bccchr.ca (Alexander Mark Weber)

0.1. Introduction

The brain is a complex system that exhibits nonlinear dynamics across multiple dimensions, including in how its activity unfolds over time. Capturing these dynamics requires more than traditional static summaries of average activity or connectivity. Instead, approaches are needed that explicitly quantify the temporal richness of brain function. One informal grouping of such approaches is temporal complexity (Figure 1). Temporal complexity metrics reflect diverse assumptions and motivations, but broadly aim to quantify regularity and irregularity in time series, including features like recurring patterns, memory, and unpredictability [1]. Temporal complexity is the most common of the complex-systems approaches to the brain (e.g., see [2] for a domain-specific review (Alzheimer’s)), and is present across scales (Figure 2), from the cellular to large-scale functional networks [3].



Source: Figures

Figure 1: A variety of approaches to nonlinear analysis of fMRI data. A Python-generated word cloud of fMRI complexity terms, weighted by number of results in PubMed. Keywords were selected from reviews of nonlinearity/complexity (including [4], [2], [5], [6], [7], and [8]).

Functional magnetic resonance imaging (fMRI) can indirectly assess temporal complexity in brain activity through the blood-oxygen level dependent (BOLD)

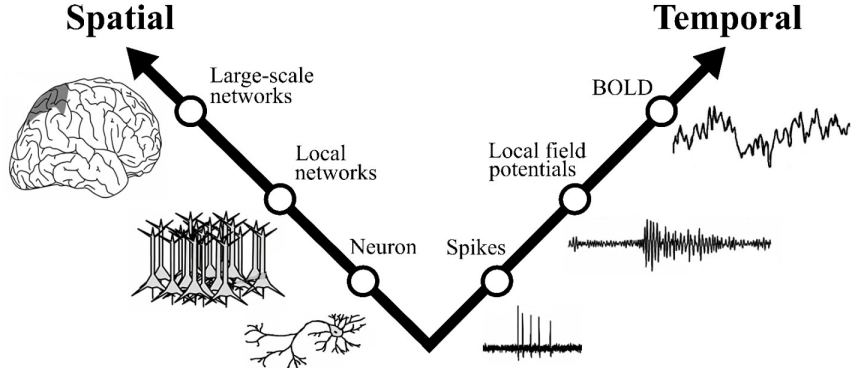


Figure 2: **The multiscale brain.** The brain displays complexity at the microscopic, mesoscopic, and macroscopic scales, both in temporal and spatial domains. Cartoons adapted from [9]; BOLD time series adapted from [10]; layout inspired by [11].

signal. Despite the fact that fMRI is traditionally considered unsuitable for rigorous temporal analyses — its time series are sampled slowly (0.5–3 s), and are relatively short in length (5–10 minutes), limiting access to fine-scale dynamics and data-hungry metrics [12] — a growing literature shows that coarse-scale dynamics remain informative. These dynamics have been linked to both cognitive and clinical states and have been reliably characterized using fMRI recordings [13, 14].

Compared to other neuroimaging modalities (reviewed in [4, 2, 5, 6, 8]), however, temporal complexity metrics are seldom used in fMRI research. This is reflected in a diffuse, unstandardized landscape in which methods are siloed across research groups, limiting accessibility and comparability. The present review aims to help bridge this gap. Going beyond previous reviews of complexity in fMRI [[13]; [xinApplicationComplexityAnalysis2021](#)], we have attempted to systematically identify all temporal complexity metrics used in fMRI research and all relevant papers that used each metric. To our knowledge, no prior review has undertaken this task at this scope.

This review also differs from previous reviews in its primary aim. Rather than summarize prior clinical and neuroscience findings (although we do include this as well), we have focused on providing guidance for clinical and cognitive researchers who wish to implement temporal complexity metrics. Many such researchers lack a background in information theory and thus face a choice: either apply temporal complexity measures without fully understanding the theoretical context — risking methodological or interpretational errors — or invest considerable time learning about a vast, interdisciplinary, and technically varied literature. Our review aims to solve this problem by serving as both a comprehensive and accessible resource for temporal complexity methods in

fMRI.

What follows is first a review of the basic concepts of various temporal complexity metrics and the history of their applications to fMRI, followed by a comparison of these metrics, and finally a discussion that explores their clinical and neuroscience findings. ## What is complexity?

Complexity is conceptualized as involving a balance between order and disorder [15]. Uniform systems (e.g., crystal lattices; sine waves) are not complex, nor are completely irregular ones (e.g., randomly moving particles; white noise); rather, complexity lies between these two extremes, combining predictability and unpredictability [1].

0.2. Variability

In order to get a sense of temporal complexity, it may help to first describe how it differs from variability. Complexity and variability are statistically distinct, yet closely intertwined. Temporal complexity and variability both describe the temporal dynamics of neurophysiological signal, with variability describing signal spread, and complexity describing within-series interactions and recurring patterns (Figure 3). A time series that is more complex is not necessarily more variable, and vice versa. Indeed, some measures of complexity explicitly make use of variability as a measure across different scales (e.g., Approximate entropy [16] or Rescaled range to measure the Hurst exponent [17]). Nevertheless, complexity and variability are closely related. Across theoretical perspectives, changes in a system (i.e. its variance) are fundamentally related to the complexity of its behaviour [18, 19, 20, 21]. Intuitively, a system cannot exhibit complex behaviour if its variability is either minimal or maximal — that is, if it is in complete stasis or fluctuates completely randomly.

A review of empirical comparisons between variability and complexity in fMRI is provided in the later section “Comparisons of All Metrics.”

0.3. Entropy measures

Entropy, in the context of time-series and brain signals, is a measure of uncertainty, irregularity, or unpredictability in a signal. It originates from information theory and statistical mechanics, but has been adapted into many specialized forms for analyzing neural dynamics. It is by far the most popular and diverse measure we encountered in our literature search, and is thus where we begin our review.

0.3.1. Shannon entropy

Shannon entropy serves as the foundation for virtually all contemporary entropy measures, and its introduction marked the birth of information theory [24]. Shannon entropy quantifies uncertainty; it can be thought of as the difficulty of predicting an observation’s value (Figure 4). Applied to a time series, it measures the minimum number of ‘bits’ needed to encode the series based on the frequency of values (Figure 5).

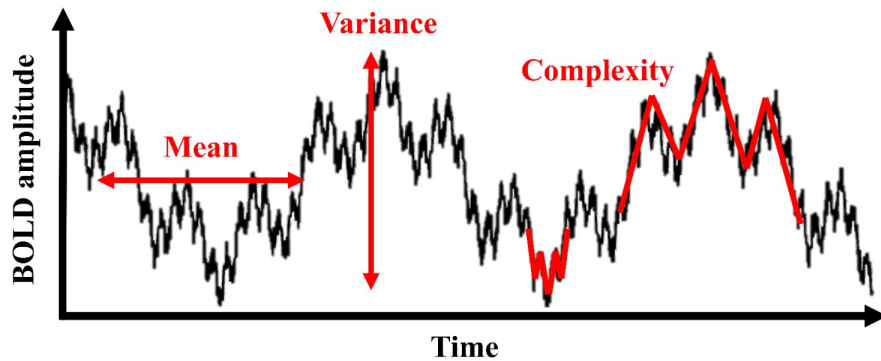


Figure 3: Conceptual comparison of the features captured by the mean (a measure of central tendency), variance (a measure of variability), and Hurst exponent (a measure of complexity; specifically long-term memory). Synthetic waveform from [22]; figure inspired by [23].

How certain are we that the next ball picked from the bucket will be red?

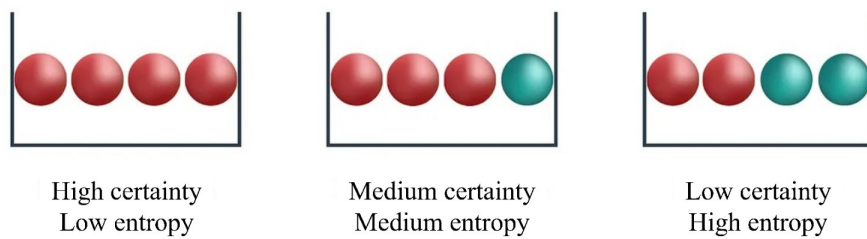


Figure 4: Shannon entropy represents uncertainty about an observation's value. Image adapted from [25].

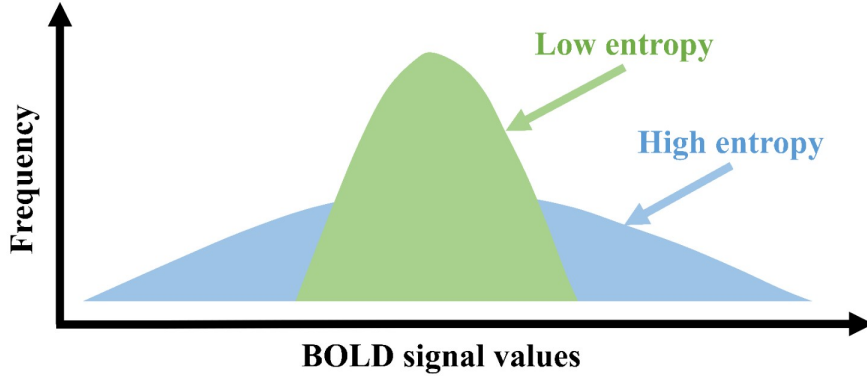


Figure 5: Shannon entropy reflects the distribution of values; a wider distribution of BOLD signal values (blue) has higher entropy, while a narrower distribution of values (green) has lower entropy

Shannon entropy can be calculated using the following equation:

$$H = - \sum_{i=1}^N p_i \log(p_i) \quad (1)$$

where H is entropy and p_i is the frequency of a given value.

Shannon entropy is seldom used to assess the temporal complexity of neuroimaging time series. Instead, it is most commonly applied to spatiotemporal properties—for example, to quantify the complexity of functional connectivity (FC) [26, 27]. This is because the classic formulation only considers frequency values, not their order. The resulting metric is poorly suited to describe how a series changes over time. Only one study, by [28], used Shannon entropy of frequency of values (details in discussion). However, several studies have applied Shannon entropy to wavelet-decomposed time series (i.e., analyzing the entropy of different frequency bins; method described in [29]), which has been shown to be an improvement over the classic formulation. For example, [30] found that Shannon wavelet entropy was able to discriminate epilepsy patients from controls, whereas classical Shannon entropy was not.

Although Shannon entropy is rarely applied with the explicit aim of describing temporal complexity, it has been used as an innovative alternative to traditional methods of analyzing event-related fMRI data. Unlike traditional methods, entropy makes no assumptions about the shape of the evoked hemodynamic response, which can improve stability and sensitivity [31, 32]. [33] were the first to apply Shannon entropy to event-related fMRI analysis. They calculated entropy

within time windows during activation and rest; the rise and fall of the entropy measure mirrored the theoretical hemodynamic response (Figure 6). Compared to traditional cross-correlation, Shannon entropy was more stable with a changing signal-to-noise ratio [33]. [34] also used Shannon entropy in event-related analysis, which allowed them to capture changes induced by photic stimulation that were missed by traditional temporal descriptors (e.g., variance). Together, these results indicate that Shannon entropy may capture features of BOLD dynamics that escape conventional temporal measures. More broadly, this demonstrates the usefulness of temporal dynamics in situations where spatial maps are unable to fully capture condition differences.

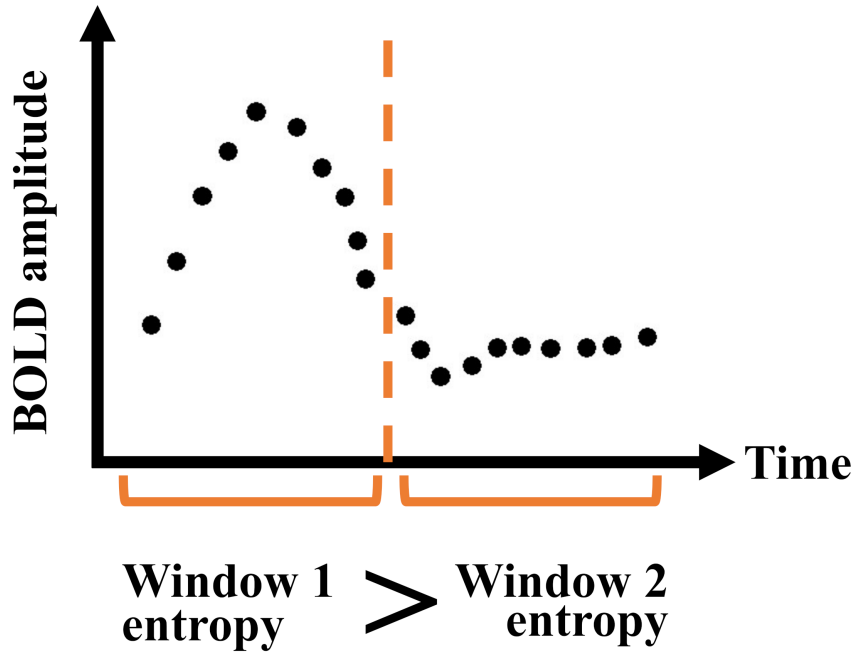


Figure 6: An example of how Shannon entropy can be used to analyze event-related data (de Araujo et al., 2003). Image stylized/recreated from de Araujo et al. (2003).

Several extensions to Shannon entropy have been introduced as alternatives to conventional methods for discriminating task conditions in event-related fMRI. A comprehensive list of these methods and their applications is as follows: Tsallis entropy (applied by [35, 36], Renyi entropy [37, 36], generalized relative entropy [38, 39], adaptive entropy rate [40], and time-lagged mutual information [41, 42, 43, 44, 45, 46]). Despite their potential effectiveness in event-related fMRI analysis, these methods have not been widely adopted, neither since they were first reviewed by [31], nor in the decade since. This may be because of their high computational demands or simply because there are better approaches to model-free hemodynamic response estimation (e.g., finite-impulse-response

models [47]. No studies have systematically evaluated whether Shannon-entropy-based analysis methods discriminate task conditions better than conventional ones, which leaves a knowledge gap.

0.3.2. Kolmogorov-Sinai entropy

In contrast to Shannon entropy, Kolmogorov-Sinai (KS) entropy takes time into account (Figure 7), allowing for application to dynamical systems [48]. As a system evolves, KS entropy quantifies the average rate at which information is produced with each new state; that is, it quantifies the difficulty of predicting future observations given past observations. Higher KS entropy implies that a higher amount of information is being introduced at each time point, meaning that the series is more unpredictable. Like Shannon entropy, KS entropy implements the intuitive notion that a broader distribution of data values should correspond to greater uncertainty.

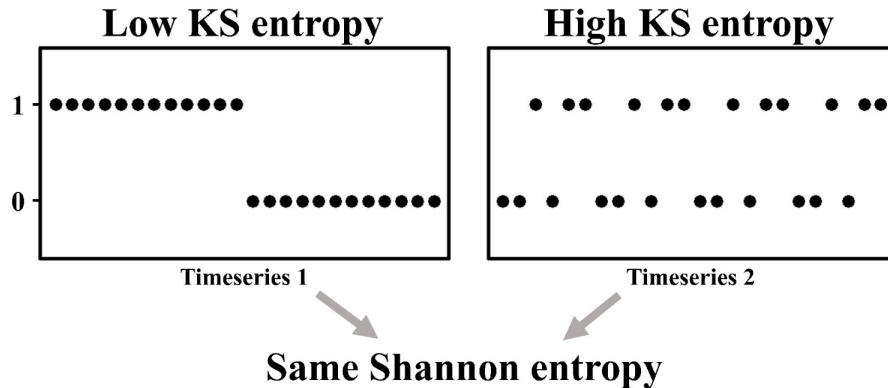


Figure 7: Because Shannon entropy only depends on the distribution of values and not their order, two sequences may look different but have the same Shannon entropy. Here, both series have the same Shannon entropy, but the series on the right has higher KS entropy. Original image

KS entropy is difficult to apply to real-world data, given that proper implementation requires exceedingly large amounts of time series data and an absence of noise [49, 16]. As such, a variety of measures have been developed as approximations for KS entropy. The following sections discuss approximations of KS entropy that have been applied to fMRI research.

0.3.3. Approximate entropy

In fMRI, nearly all approximations of KS entropy can trace their historical lineage to approximate entropy (ApEn) [49]. First used on cardiovascular time series and later adapted for neuroimaging [16, 50], ApEn quantifies the probability that sequences of similar patterns in a time series will remain similar when

sequence length is increased. A higher value of ApEn signifies that the signal contains fewer repeating patterns—that is, greater complexity.

In the calculation of ApEn, each sequence is counted as matching itself [16]. This nuance leads to two limitations. First, it causes ApEn to be lower than expected for shorter time series [16]. This is because counting self-matches inflates the estimation of regularity, and this over-inflation is more prominent for short series. Shortening datasets (e.g., by using one fMRI run instead of two) may change ApEn despite identical patterns. Second, ApEn lacks relative consistency, meaning that comparisons between datasets can be affected by the choice of time-window and tolerance parameters (i.e., if ApEn is higher for one dataset than another using one set of parameters, we would expect this to remain true for other choices of parameters, but this is not the case; [16]).

Given these limitations, ApEn is rarely used to characterize temporal complexity in fMRI. In most fMRI studies, ApEn is reported only alongside other entropy-based measures — such as sample entropy (SE) or fuzzy approximate entropy — and therefore these applications are included in our “Comparisons of All Metrics” section. Two ApEn studies that do not appear in that section are [51] and [52]; both report clinical findings that align with the broader complexity literature, and we summarize these in the Discussion.

0.3.4. Sample entropy

Sample entropy (SE) was developed to correct ApEn’s limitations [16]. The difference between the calculation of SE and that of ApEn is that SE doesn’t count self-matches in the conditional probability, which corrects the two limitations described in the ApEn section [16] (for an example in fMRI, see [53]). In addition to these advantages, SE is a better approximation of KS entropy and is simpler to compute [16]. Accordingly, SE is more widely used than ApEn in fMRI and can be computed using the toolboxes BENtbx <https://github.com/zewangnew/BENtbx>; e.g., Wang et al., 2014 (e.g., [54]) or Complexity Toolbox <http://loft-lab.org/index-5.html>; e.g., Zhang et al., 2021 (e.g., [55]). SE is most often called “brain entropy” (BEN) [54]; however, because BEN can also refer to Shannon entropy [56], we elected to use the term SE in this review.

To calculate SE, the user specifies two parameters: the time window m and the tolerance scale r . m is the number of values to be analysed at a time, and r is the multiplied by the standard deviation (SD) of the series to obtain the tolerance. SE is equal to the negative average natural logarithm of the conditional probability that two sequences that are similar (i.e., within the tolerance) for m points will stay similar for $m + 1$ points [16]. Because conditional probability is between 0 and 1, SE will always be positive. When the time series is highly regular (i.e., when similar runs remain similar), SE is low; when the time series is irregular, SE is high [49]. See Figure 8 for a conceptual explanation, Figure 9 for a computational explanation, and [57] for a tutorial. For a detailed guide to selecting m and r , see Appendix A1 and Figure A1.

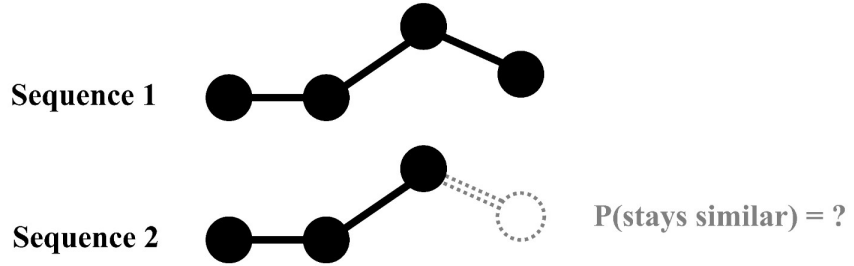


Figure 8: **Conceptual explanation of SE.** SE represents the probability that similar sequences will stay similar. Original image.

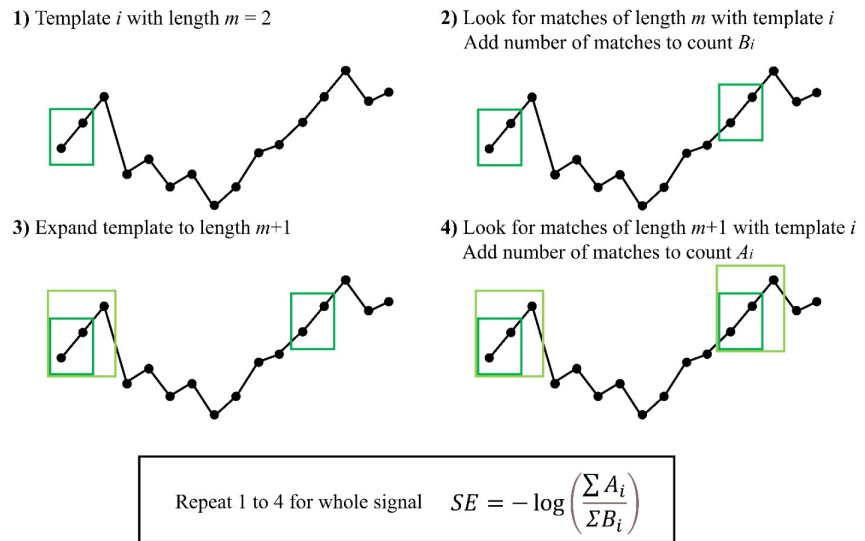


Figure 9: **An example SE calculation with $m = 2$.** Original image, except for time series (black dots/lines) which is adapted from [58].

What is the minimum number of timepoints needed for SE? In general, more timepoints improve results. For example, using simulated data, [12] found that SE accuracy and precision increased fairly linearly from the shortest to longest series tested (32 to 32,768). [59] (Figure 10) observed strong (albeit non-significant) correlations between reliability and series length, including a slow increase in split-half correlation from the shortest to longest series tested (100-800), along with a steady increase in test-retest correlation that plateaued around 500. Highlighting that the relationship between length and reliability is dataset-dependent, they found differences in rest versus task data (for a wide variety of tasks, including cognitive, motor, and social). As for the lower limit of length, [53] identified a lower bound of 97 timepoints; for series shorter than 97, SE could still be calculated, but with a narrower range of m - and r -values. [60] found that SE discriminated between young and old adults in series as short as 85 in a small ($n = 20$) cohort. Again highlighting that length limitations are dataset-dependent, [60] found that more data points were needed in a larger ($n = 86$) cohort (potentially because the smaller cohort had low inter-individual variability).

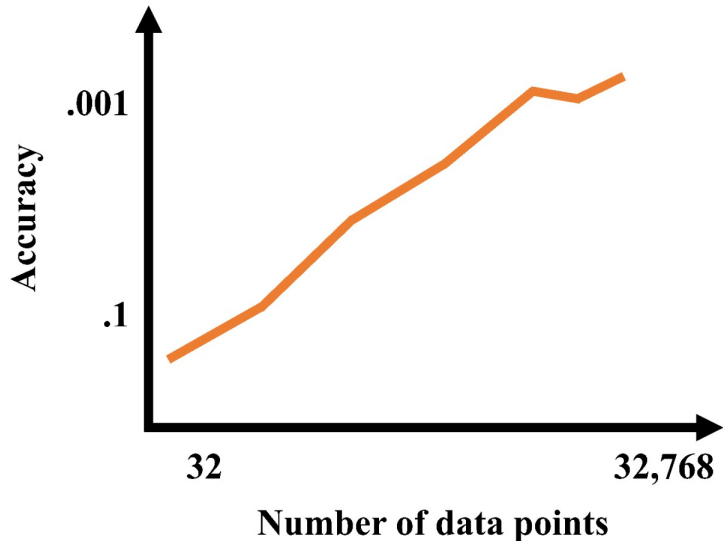


Figure 10: SE accuracy (and precision, not shown) increase with increasing series length. Figure stylized based on results from Wehreim et al. (2024).

Several innovations to SE have been made in recent years. [61] introduced “cross” SE, a method for comparing multiple SE maps which can be applied to make comparisons between subjects, sessions, scan times, or regions. Thus far, cross entropy has been used to show a decoupling between the (across-subject) mean and variance of SE across different brain regions [61]. [62] pioneered dynamic SE, wherein SE is estimated for every segment of a sliding window. Despite its name, dynamic SE is not designed to be used to track changes in SE

over the course of a run; instead, SE for each segment is combined into a final run mean. In a sample of 862 subjects, [62] found minimal differences between static (traditional) and dynamic SE.

Table 1 includes a complete summary of fMRI-SE studies and their findings.

Table 1: **fMRI-SE and MSE studies.** An attempt to gather all published fMRI studies that have used SE or MSE, some stats, and the main findings. Main findings are more nuanced than how we have reported them here; we have attempted to condense the findings as succinctly as possible. Excludes analyses that do not meet the definition of temporal complexity used in this review: SE of the spatial map, SE of dynamic functional connectivity, and SE computed on synthetic data. For sample size and age, commas separate cohorts. \uparrow / \downarrow = Higher / lower; ACC = anterior cingulate cortex; AD = Alzheimer's; ADHD = attention-deficit hyperactivity disorder; ASD = autism spectrum disorder; corr. w/ = Correlated with; diff. = difference; DLPFC dorsolateral prefrontal cortex; DMN = default mode network; DPN = diabetic peripheral neuropathy; FG = frontal gyrus; FPN = frontoparietal network; HC = Healthy controls; MCI = mild cognitive impairment; MDD = major depressive disorder; MOFC = medial orbitofrontal cortex; MTL = medial temporal lobe; n.s. = not significant; OA = older adults; OCD = obsessive-compulsive disorder; OFC = orbitofrontal cortex; oppositional defiance disorder = ODD; PFC = prefrontal cortex; SMA = supplementary motor area; TPJ = temporal parietal junction; VMPFC = ventromedial prefrontal cortex; YA = young adults.

Reference	Sample	Age (years)	Sample (s)	Volume	Rest/task	MSE)	Method	Parameter	Results		
									or		
							min -	max;	TR	(SE	or
[63]	ASD	8-14	2.5,	120,	rest	SE	$m =$	ASD: \uparrow SE in left			
		45,	2	152			$2,$	angular gyrus,			
	HC						$r = 0.46$	superior parietal			
		45						lobule, right			
								inferior temporal			
								gyrus; \downarrow SE in			
								superior FG.			
[64]	Cocaine	42 ± 20,	2	180	rest	SE	$m =$	Cocaine			
		4, 40					$3, r =$	addiction: \uparrow SE			
	HC	± 5					0.6	in VMPFC,			
		19						OFC, DLPFC,			
								ventral striatum,			
								basal ganglia,			
								visual cortex,			
								parietal cortex.			
[65]	ASD	1-1.5	2	240	rest	SE	$m =$	ASD: \uparrow SE in			
		42,					$3, r =$	right inferior FG.			
	HC						$=$				
		42					0.6				

		Age (mean ± sd or min - max; TR			Method (SE or			
Reference	Sample	years)	(s)	Volume	Rest/task	MSE)	Parametric	Results
[66]	26	25- 45	1.5	360	rest	SE	$m =$ $3, r$ $=$ 0.6	Acute alcohol intake: Within regions with reductions in regional signal variability, ↓ SE in bilateral middle FG, right superior FG.
[67]	YA 44, OA 43	18- 31, 63- 81	2	240	rest	SE	$m =$ $3, r$ $=$ 0.6	Intranasal oxytocin: In left TPJ, SE ↑ in YA, ↓ in OA.
[68]	280	38- 44 weeks post- men- strual age	0.392	2300	rest	SE	$m =$ $3, r$ $=$ 0.3	Postnatal age ↑ corr. /w SE in sensorimotor- auditory cortex, association cortex, right rolandic operculum. Gestational age ↓ corr. /w SE in sensorimotor- auditory cortex and association cortex, and ↑ corr. /w SE in right rolandic operculum. Pre-term infants: ↑ SE in visual-motor cortex.
[1]	Dataset A Dataset B	19- 25, 52, 18- 19 40	2, 2	150, ?	rest	SE	$m =$ $2, r$ $=$ 0.3	SE ↓ with increasing propofol sedation.

Reference	Sample	Age (mean ± sd or min - max; TR	Volume	Rest/task	SE	Method (SE or		Parameters	Results
						m =	n =		
[69]	OCD 74, HC 93	18- 60	2	200	rest	SE	$m = 3, r = 0.2$	SE map did not match brain structure. No difference between OCD and HC, or between genders.	
[70]	Concuss 28, HC 379	9eh7	2	180	rest	SE	$m = 3, r = 0.6$	Concussion vs HC classification: Most important region for classification was subcallosal cortex.	
[71]	Dataset18- A 50, 50, Dataset21- B 50 130	18- 50, 50	2, 2	288, varies	rest, task	SE	$m = 2, r = 0.5$	Interoceptive > Exteroceptive > Mental ROIs for all of rest and task. Rest > Task.	
[72]	MDD 85, follow- up 30, HC 45	44 ± 85, 41 ± 14, 43 ± 14, 12	2	240	rest	SE	$m = 3, r = 0.6$	MDD: ↓ SE in MOFC/subgenual-ACC; ↑ SE in motor cortex.	
[73]	107	31 ± 14	2	240	rest	SE	$m = 3, r = 0.6$	Cerebral blood flow ↑ corr. /w SE in OFC, posterior inferior temporal cortex. n.s. direct relationship between SE and gender.	

		Age (mean ± sd or min - max; TR	Method (SE or	Parameter	Results
	Reference	Sample years) (s)	Volume rest/task MSE)		
[74]		1206 29 ± 4	0.72	1200 rest SE	$m = 3, r = 0.6$ n.s. relationship between SE and heart rate. Cognition corr. /w SE ↓ in fronto-parietal cortex, ↑ in sensorimotor system.
[75]	ASD 20, HC 17	10- 18, 8-18 17	2	180 rest SE	$m = 1-4, r = 0.05-0.8$ ASD: n.s. diff. in SE. SE ↑ corr. /w global efficiency of structural connectome and age, ↓ corr. /w behavioural ASD score.
[76]		892 18- 35	3	120 rest SE	$m = 3, r = 0.6$ Intelligence ↑ corr. /w SE, especially in PFC, inferior temporal lobes, cerebellum.
[77]	Classical trigem- inal neu- ral- gia 85, HC 79	56 (in- terquar- tile range 13), 55 (in- terquar- tile range 14)	2	240 rest SE	$m = 3, r = 0.6$ Classical trigeminal neuralgia: ↑ SE in thalamus and brainstem, ↓ SE in inferior semilunar lobule.

Reference	Sample	Age (mean ± sd or min - max; TR)	Volume	Rest/task	SE	$m =$ $3, r$ = 0.6	Method (SE or		Results
							NSE	Parametric	
[78]	386	17- 27	242	rest	SE				Divergent thinking ↑ corr. /w SE in left dorsal ACC/pre-SMA, left DLPFC. Fluency, flexibility, and originality ↑ corr. /w SE in left inferior FG and left middle temporal gyrus.
[79]	HC 54, Sig- nifi- cant mem- ory con- cern 27, early MCI 58, late MCI 38, AD 34	65- 95, 65- 83, 56- 89, 57- 88, 56- 87	3	140	rest	SE	$m =$ $3, r$ = 0.6		Aging in HC: ↑ SE. Aging in AD: ↓ SE. In AD SE ↑ corr. /w impairment. Cerebrospinal fluid A depositions ↓ corr. /w SE in HC, while ↑ corr. in AD. Important regions: DMN, MTL, PFC.

Reference	Sample	Age (mean ± sd or min - max; TR)	Volume (s)	Rest/task NISE)	Parameter	Results	
						Method (SE or	
[54]	Small co- hort 16, Large co- hort 1049	25 ± 5, 27 ± 11	3, 3, 0.75- 3	220, 220, 72- 395	task, rest	SE $m =$ $3, r =$ $=$ 0.6	Atlas of SE: SE reproduces known network parcellations.
[80]	Chronic fa- tigue syn- drome 43, HC 26	47 ± 12, 43 ± 14	0.798	1100	task	SE $m =$ $3, r =$ $=$ 0.2	Chronic fatigue syndrome: ↓ SE in 10 of 50 regions.
[81]	TBI only 60, TBI with psy- chogenic nonepilep- tic seizures 21, TBI with epilep- tic seizures 56	38 ± 12, 39 ± 12	1	1200	task	SE $m =$ $3, r =$ $=$ 0.6	TBI with psychogenic nonepileptic seizures: SE ↓ corr. /w depression. TBI only, TBI with epileptic seizures: n.s. correlation between SE and depression. Across all groups: ↓ SE in FPN.

Reference	Sample	Age (mean ± sd or min - max; TR)	Volume (s)	Rest/task MSE)	Parameter	Results	Method (SE or
							m =
[82]	60	23 ± 2	?	rest	SE	$m = 3, r = 0.6$	Caffeine intake: ↑ SE across cerebral cortex, with the highest increase in lateral PFC, DMN, visual cortex, motor network.
[83]	31	19-25	3	100 task, rest	SE	$m = 3, r = 0.6$	Task vs rest: n.s. diff. in SE.

Reference	Sample	years)	(s)	Volume	Rest/task	SE	$m =$	Method	(SE	Results	
										or	Results
[84]	Marijuana de- pen- dence 59, HC matched to mar- i- juana group 59, Nico- tine de- pen- dence 34, HC matched to nico- tine group 34, Alco- hol de- pen- dence 35, HC matched to alco- hol group 34	0.72	1200	rest	SE	$m =$	3, r =	Marijuana dependence: ↑ SE. Nicotine dependence: ↑ SE. Alcohol dependence: ↑ SE.	NISE)	Parameter	

Reference	Sample	years)	(s)	Volume	Rest/task	SE	$m =$	Method (SE or	Age (mean \pm sd or min - max; TR	Results
[85]	3 cohorts	21 ± 2, 31 of HC:	2.5, 1.75 27 ± 29, 35, 36	197	rest	SE	$m =$ $2, r =$ $=$ 0.25	Reliability (test-retest): Poor to fair to good.		
[86]	412	22- 35?	0.72	1200?	rest, task	SE	$m =$ $3, r =$ $=$ 0.6	Task (emotion, language, sensorimotor, gambling/risk-taking, relational processing, social processing, combination working memory/category-specific representation): Regions predicted to be active based on the literature < Regions predicted to be less relevant. Amplitude ↓ corr. /w SE in task but not rest.		

Reference	Sample	Age (mean ± sd or min - max; TR)	Volume	Rest/task	SE	$m =$ $3, r$ $=$ 0.6	Method (SE or NISE)		Parameters	Results
							Volume	Rest/task	NISE)	
[87]	MDD 46, HC 32	28 ± 2 9, 27 ± 10	240	rest	SE	$m =$ $3, r$ $=$ 0.6	MDD: ↓ SE across whole brain and in bilateral thalamus, bilateral insula, bilateral putamen, left caudate, right inferior FG. Depression score ↓ corr. /w SE.			
[88]	YA 577, OA 424	29 ± 0.72, 4, 61 ± 15	478, 478	rest	SE	$m =$ $3, r$ $=$ 0.6	n.s. relationship between SE and pain intensity.			
[89]	2415	8-89	0.72	488	rest	SE	$m =$ $3, r$ $=$ 0.6	Increase in SE from childhood to older adulthood		
[90]	Chronic pain 13132, HC 18173, Non- chronic pain 4922	64 ± 8, 64 ± 8, 63 ± 8	0.735	490	rest	SE	$m =$ $3, r$ $=$ 0.6	Chronic pain: ↑ SE.		

Reference	Sample	Age (mean ± sd or min - max; TR)	Volume	Rest/task	SE	$m =$	Results	
							MSE	Parameter
[91]	ADHD ODD OCD	10 ± 61, 1, 10 ± 1, 38, 10 ± 1, 1, 10 48, ± 1, co- 10 ± 1 mor- bid ADHD/ODD/OCD 833, HC 269	varied varied rest	rest	SE	$m =$ $2, r$ = 0.3	In executive function networks: Comorbid-free ADHD < HC, comorbid-free ODD < HC, comorbid-free OCD = HC, ADHD < HC, within comorbid ADHD/ODD/OCD: ADHD < HC.	
[92]	100	22- 36	0.72	1200, ~400	rest, task	SE	$m =$ $3, r$ = 0.6	Atlas of SE at rest and task. SE task < Rest.
[93]	86	19- 85	2	133	rest	SE	$m =$ $2, r$ = 0.3	No effect of age or sex.
[94]	Chronic smoking	19- 58, 21- 68, 51	2	150	rest	SE	$m =$ $3, r$ = 0.6	Chronic smoking: \downarrow SE in right limbic area and frontal region.
[95]	1087	6-30	varied	varied	rest	SE	$m =$ $1, r$ = 0.15	n.s. diff. between ASD and HC.

Reference	Sample	Age (mean ± sd or min - max; TR)	Volume	Rest/task	SE	$m =$ $r =$	Results	
							MSE	Parameter
[96]	Stroke 19, OA 19, YA 20	65 ± 2 2, 66 ± 2, 25 ± 1 20	180	rest	SE	$m =$ $2, r =$	YA < OA. n.s. diff. between stroke patients and HC. n.s. corr. /w hypoperfusion in perilesional tissue.	
[97]	Bipolar-II 19, HC 17	15 ± 2 2, 14 ± 2 17	?	rest	SE	$m =$ $3, r =$	Bipolar-II: ↑ SE in parahippocampal gyrus and inferior occipital gyrus.	
[98]	MCI 44, HC 40	75 ± 2.2 8, 77 ± 7	164	rest	SE	$m =$ $= 3,$ $r = 0.6$	MCI: ↓ SE in left middle temporal gyrus.	
[99]	Depression (14 treat- ment), HC 20	33 ± 2.5 9, 30 ± 8	100	rest	SE	$m =$ $= 3,$ $r = 0.6$	Depression: ↑ SE in left DLPFC and limbic system; increase can be reversed through treatment.	
[100]	AD 26, HC 26	73 ± 3 8, 75 ± 6	140	rest	SE	$m =$ $3, r =$	AD: ↑ SE in middle temporal gyrus and precentral gyrus. Network connectivity more ↓ corr. /w SE in AD vs HC.	
[101]	410	22- 36	0.72	1200	rest	$m =$ $2, r =$	Reliability (test-retest): Good.	
						$=$ 0.5		

Reference	Sample	Age (mean ± sd or min - max; TR	Volume	Rest/task	SE	Method (SE or	Results	
							years)	(s)
[102]	High-grade glioma 85, Low-grade glioma 76, HC 51	47 ± 2 15	220- 301	rest	SE	$m =$ 1-3, $r =$ 0.7	Glioma: ↓ SE.	
[103]	862	22- 37	0.72 1200	rest, task	SE	$m =$ 3, $r =$ 0.6	Rest SE ↓ corr. /w magnitude of (de)activation in regions activated by task.	
[104]	176	29 ± 3	varies varies	rest, movie	SE	$m =$ 3, $r =$ 0.6	Identified regions where neurotransmitters (5HT1a, 5HTT, D1, D2, DAT, H3, MU, NMDA, VACHT, 5HT1b) contribute to structure- function coupling (incl. visual cortex, temporal cortex, paracentral lobule, DLPFC).	
[105]	20	42- 57	2 160	rest	SE	$m =$ 2, $r =$ 0.3	Seafarers: ↑ SE in orbital-FG and superior temporal gyrus, ↓ SE in cerebellum.	

Reference	Sample	Age (mean ± sd or min - max; TR)	Volume	Rest/task	SE	$m =$ $3, r$ $=$ 0.6	Method (SE or MSE)		Parameters	Results
							Rest	MSE		
[106]	24 years	58- 77	2	~151	rest	SE			$m =$ $3, r$ $=$ 0.6	YA > OA (longitudinal). Earlier-born > Later-born (cohort effect). With age, SE decreases faster in primary and intermediate networks than in higher-order association networks.
[107]	ADHD 12 ± 74, 2, 12 HC ± 2 69	varies	varies	rest	SE	$m =$ $2, r$ $=$ 0.2				SE (and phase synchronization, IQ, age, ADHD diagnosis, and head motion) can be input into a predictive model to predict inattention and impulsivity.
[108]	Sham 23 ± 18, 3, 23 rTMS ± 3 30	2	180	rest	SE	$m =$ $3, r$ $=$ 0.6				rTMS to left DLPFC: ↓ SE in MOFC/subgenial- ACC.
[109]	Stroke 35- 23, 80 HC 19	2	240	rest	SE	$m =$ $2, r$ $=$ 0.3				Stroke: ↓ SE in contralesional precentral gyrus, bilateral dorsolateral FG, bilateral SMA.

Reference	Sample	Age (mean ± sd or min - max; TR)	Volume (s)	Rest/task MSE)	Method (SE or	Results		
						$m =$ $3, r$ =		
[110]	176	22- 36	1	900, 921, 918, 915, 901	rest, movie	SE	Movie < Rest in sensory cortex. Movie > Rest in association cortex. Higher inter-scan reliability in movie (esp. in vmPFC and PCC) than in rest.	
[111]	41	23 ± 4	2	240	rest, task	SE	$m =$ $3, r$ =	Rest < Task in DLPFC, TPJ, posterior cingulate cortex, precuneus. Rest > Task in visual cortex. Rumination < Sad memory in visual cortex. Distraction < Sad memory in posterior cingulate cortex/precuneus. Distraction < Rumination in posterior cingulate cortex/precuneus.

Reference	Sample	Age (mean ± sd or min - max; TR)	Volume (s)	Rest/task (SE)	$m =$ r	Method (SE or NISE)	Parameters	Results
								Rest task
[112]	RRMS	20- 34, HC 21- 34	2 58, 58	240 rest	SE =	$m =$ r	Relapsing- remitting multiple sclerosis (RRMS): ↑ SE in SMA, right PFC, right angular gyrus; ↓ SE in right precentral operculum, left middle temporal gyrus, bilateral parahippocam- pus, brainstem, right posterior cerebellum. Disease severity and tissue damage ↑ corr. /w SE.	
[113]	ADHD	30 ± 17, HC 10, 30 ± 13, 8	3 100	rest	SE =	$m =$ r	ADHD: ↓ SE across whole brain and in frontal and occipital lobes. Symptoms ↓ corr. /w SE.	

Reference	Sample	Age (mean ± sd or min - max; TR)	Volume	Rest/task	Method (SE or NISE)	Parameter	Results
[114]	Schizophrenia	24 years 43, 14, HC 35 ± 59 11	150	rest	SE	$m =$ $3, r$ $=$ 0.6	Schizophrenia: ↓ SE in right middle PFC, bilateral thalamus, right hippocampus, bilateral caudate. Schizophrenia: ↑ SE in left lingual gyrus, left precuneus, right fusiform face area, right superior occipital gyrus. In left cuneus and middle occipital gyrus, symptoms ↓ corr. /w SE. In right fusiform gyrus and left insula, age of onset ↓ corr. /w SE.
[115]	989	29 ± 0.72 4	1200	rest	SE	$m =$ $3, r$ $=$ 0.6	SE ↓ corr. /w gray matter volume and surface area (in lateral frontal and temporal lobes, inferior parietal lobules, and precuneus), n.s. relationship /w cortical thickness.

Reference	Sample	Age (mean ± sd or min - max; TR)	Volume	Method		Parametric Results	
				Rest	/task (SE or MSE)		
[60]	YA 10, OA 10, YA 43, OA 43	22 ± 2 3, 70 ± 9, 29 ± 9, 59 ± 10	85- 128	rest	SE	$m = 2, r = 0.3$ YA > OA in frontal and parietal lobes. SE discriminated between YA and OA across series lengths (N = 85-128) in a small, low-variability cohort, but only in long series (N = 128) in a large, high-variability cohort.	
[116]	1642	18- 65	varies	varies	rest	SE	$m = 2, r = 0.2$ Females > Males (largest effect in DMN), difference associated with expression of genes that were enriched in estrogen-signaling pathway.
[117]	1096	29 ± 4	0.72	varies	rest, task	SE	$m = 1, r = 0.6$ Task < Rest in peripheral cortical area. Task > Rest in centric part of sensorimotor and perception networks.

Reference	Sample	Age (mean ± sd or min - max; TR)	Volume	Rest/task	SE	$m =$ $3, r$ $=$ 0.6	Method (SE or NISE)		Parameters	Results
							SE	NISE		
[62]	862	22- 37	0.72	1200	rest					SE ↓ corr. /w activity in default mode and executive control networks. SE ↑ corr. /w age in prefrontal executive control network and frontal-temporal-parietal DMN. Women > Men in visual cortex, motor area, some parts of precuneus. SE ↓ corr. /w years of education, fluid intelligence, and performance during working memory/language/relational tasks in DMN and executive control network.
[118]	44	23 ± 2	2.53	240	rest	SE	$m =$ $3, r$ $=$ 0.6			SE ↓ corr. /w progesterone in FPN and limbic network. SE ↑ corr. /w impulsivity in left DLPFC.
[119]	42	18- 45	0.8	600	rest	SE	$m =$ $3, r$ $=$ 0.3			Smoking: ↑ SE. rTMS in DLPFC reduced resting SE in insula and DLPFC.

	Age (mean ± sd or min - max; TR		Method (SE or		Results		
Reference	Sample years)	(s)	Volume	Rest/task	MSE)	Parameter	Results
[120]	66	9-37	?	?	rest	SE	?
							SE ↑ corr. /w PCA components.
[121]	cTBS 18, LF- rTMS 23	23 ± 2, 3, 26 ± 3 1.25	180, 600	rest	SE	$m = 3, r = 0.6$	Continuous TBS (cTBS) to left DLPFC: ↑ SE in MOFC. Low-frequency rTMS (LF-rTMS) to left DLPFC: ↑ SE in MOFC/subgenual- ACC, putamen. LF-rTMS to left TPJ: ↑ SE in right TPJ. LF-rTMS to L occipital cortex: ↓ SE in the posterior cingulate cortex.
[36]	Short- and long- term scans 25, multi- band EPI 22, eyes open or closed	29 ± 2, 9, 32 ± 1.4, 12, 22 ± 2 2	195, 0.645, 430, 2.5, 180	rest	SE	?	Reliability (inter- and intra- scan, varying TR, eyes-open vs eyes-closed) for 10 networks: Fair to high.
							48

	Age (mean ± sd or min - max; max; TR	Method (SE or	Results	
Reference	Sample years)	Volume (s)	Rest/task MSE)	Parameter
[122]	Schizophrenia 13, 12, HC 42 ± 16 12	2.5	244 task SE	$m = 2, r =$ $= 0.32$
[123]	HC 36 ± 1.5 640, 13, Schizophrenia 16e ± 13, 13, 288, 37 ± Bipolar 13 183	200	rest SE	$m = 1, r =$ $= 0.32$
[124]	16 28 ± 2 7	300	rest SE	$m = 3, r =$ $= 0.6$
[125]	35 28 ± 2 ?	450	task SE	$m = 2, r =$ $= 0.4$

Reference	Sample	Age (mean ± sd or min - max; TR)	Volume	Rest/task	SE	Method (SE or MSE)	Parameters	Results
								years) (s)
[126]	CPI 29, HC 29	43 ± 2 11, 42 ± 12	240	rest	SE	$m =$ $3, r$ $=$ 0.6	Chronic primary insomnia (CPI): ↑ SE in central part of DMN, anterior regions of task-positive network, hippocampus, basal ganglia; ↓ SE in right postcentral gyrus and right temporal-occipital junction.	
[127]	288, 183	36 ± 1.5 13, 37 ± 13	200	rest	SE	$m =$ $1, r$ $=$ 0.32	Bipolar > Schizophrenia, largest differences in visual domain, temporal domain, somatomotor domain, high-cognitive domain.	
[128]	GAD 38, HC 37	40 ± 2.4 2, 28- 47	217	rest	SE	$m =$ $3, r$ $=$ 0.6	Generalized anxiety disorder (GAD): ↑ SE in right middle occipital gyrus and right inferior occipital gyrus.	

Reference	Sample	Age (mean ± sd or min - max; TR)	Volume	Rest/task	MSE	Parameter	Results	
							SE	Method (SE or
[129]	rTLE	28 ± 2 31, 7, 28 HC ± 5 33	180	rest	SE	$m =$ $3, r$ $=$ 0.6	Right temporal lobe epilepsy (rTLE): ↑ SE in right middle temporal gyrus and inferior temporal gyrus; ↓ SE in right middle FG and left SMA.	
[130]	HC 156, 7, 76 HC ± 7, to 74 ± MCI 8, 73 16, ± 8, MCI 76 ± 80, 8 MCI to AD 20, AD 23	72 ± 3 200	140- 200	rest	SE, MSE	$m =$ $2, r$ $=$ $0.3,$ scale fac- tors $=$ $1-4$	Fine-scale MSE: Faster longitudinal ↓ in HC-to-MCI than scale in HC (in PFC and lateral occipital cortex). Coarse-scale MSE: Faster longitudinal ↓ in AD than in HC (in various frontal and temporal regions).	
[53]	354	21- 89	2.5	200	rest	SE, MSE	$m =$ $1, r$ $=$ $0.35;$ $m =$ $2, r$ $=$ $0.5;$ $m =$ $3, r$ $=$ 0.7	Age ↓ corr. /w mean MSE.

Reference	Sample	years)	(s)	Age (mean ± sd or min - max; TR	Volume	Rest/task	MSE)	Parametric	Results
									Method (SE or
[131]	Small co- hort Large co- hort 272	24- 34, 21- 10, 50	2.2,	~800, rest 300?	SE, MSE	$m =$ $2, r$ =	ADHD/Bipolar/Schizophrenia diff. from HC across regions and atlases (mixed directions) for 1-10 SE and some scales of MSE.		
[59]	330	22- 36	varies	varies	rest, task	SE, MSE	$m =$ $2, r$ = 0.2; $m =$ $3, r$ = 0.2, scales = 1- varies	Reliability (split-half, test-retest correlations); Moderate to good. Dependence on scan length: Low.	
[12]	20	20- 30	0.645	900	rest	SE, MSE	$m =$ $2, r$ = 0.5, scales = 1-10	MSE can be accurately estimated across discontinuous segments. Dependence on scan length: Low.	

	Age (mean ± sd or min - max; TR			Method (SE or			Results
Reference	Sample	years)	(s)	Volume	Rest/task	MSE)	Parameters
[132]	147	73 ± 8	3	197	rest	SE, MSE	$m = 2, r = 0.5,$ $scales = 1-6$ Classifier (HC vs AD) performance was similar for SE, mean MSE, and tau-PET. Salience network regions were most important for SE; dorsal attention regions were most important for MSE.
[133]	Parkins	64' ± 8, 64	0.75	~495	rest	MSE	$m = 1, r = 0.35,$ $scales = 1-10$ Depression in Parkinson's: ↓ mean MSE in posterior cingulate gyrus, SMA, cerebellum.

Reference	Sample	Age (mean ± sd or min - max; TR)	Volume	Rest/task	MSE	$m =$ $1, r$ $=$ $0.35,$ $scales$ $=$ $1-4$	Method (SE or MSE)		Parameters	Results
							Volume	Rest/task	MSE	
[134]	168	60- 90	3	140	rest					Scale-1 MSE: HC > Amnestic MCI (aMCI) > AD in hippocampus, middle FG, intraparietal lobe, superior FG. Scale-4 MSE: HC < aMCI < AD in middle FG and middle occipital gyrus. Cognitive functions ↑ corr. /w fine-scale MSE, while ↓ corr. /w coarse-scale MSE.

Reference	Sample	Age (mean ± sd or min - max; TR)	Volume	Rest/task	MSE	$m =$	Method	
							Parameter	Results
[55]	Schizophrenia 50, Bipo- lar 49, HC 49	21 years 50 49, 49	152	rest	MSE	$m =$ 2, $r =$ $0.3,$ $=$ $1-5$	Schizophrenia and bipolar: ↓ mean MSE across whole brain and in calcarine fissure, precuneus, inferior occipital gyrus, lingual gyrus, cerebellum; ↑ mean MSE in median cingulate, thalamus, hippocampus, middle temporal gyrus, middle FG. Differences between schizophrenia and bipolar in precuneus and inferior occipital gyrus.	

Reference	Sample	Age (mean ± sd or min - max; TR)	Volume	Rest/task	MSE	$m =$	Method	
							(SE or MSE)	Parameter
[135]	Progressive supranuclear palsy clear palsy 94, HC 64	65 ± 2	305	rest	MSE	$m =$ 1, r = 0.35, scales = 1-3 for dataset 1; 1-4 for dataset 2	Progressive supranuclear palsy: ↓ mean MSE in one of two datasets. MSE ↑ corr. /w the fractional occupancy component that differed between people with progressive dataset supranuclear palsy and controls.	
[136]	HC 8, MCI 9	74 ± 2 4, 79 ± 8	720	task	MSE	$m =$ 2, r = 0.2, scale = 6	MCI: ↓ scale-6 MSE. Age: ↓ scale-6 MSE.	
[137]	MDD 35, HC 22	68 ± 2 6, 69 ± 6	180	rest	MSE	$m =$ 2, r = 0.6, scales = 1-5	MDD: ↑ scale-2 MSE in left FPN.	

Reference	Sample	Age (mean ± sd or min - max; TR)	Volume	Rest/task	MSE	Method		Parameters	Results
						(s)	(SE or MSE)		
[138]	OA 99, YA 56	81 ± 2.5 5, 28 ± 4	200	rest	MSE	$m = 1, r = 0.35,$ scales = 1-5	Cognitive score ↑ corr. /w MSE in 26 of 33 regions. OA (vs YA): ↓ MSE in left olfactory cortex, right posterior cingulate gyrus, right hippocampus, superior occipital gyrus, left caudate.		
[139]	10	24- 34	2.2	136	rest	MSE	$m = 2, r = 0.5,$ scales = 1-30	Atlas of MSE: MSE reproduces known network parcellations.	
[140]	44	25 ± 4	2.5	3000	sleep	MSE	$m = 1, r = 0.35,$ scales = 1-3	Deeper sleep: ↓ fine-scaled MSE, consistent coarse-scaled MSE.	

Reference	Sample	Age (mean ± sd or min - max; TR)	Volume	Rest/task	MSE	Method		Parameters	Results
						(SE or =	(MSE)		
[141]	Schizophrenia 105, 9, 43 HC ± 11 210	18 years 2.5	200	rest	MSE	m = 1, r = 0.35(SC): ↓ SE at all scales = 1-5	Schizophrenia scales in inferior temporal gyrus, middle FG, superior FG, left SMA, cerebellum posterior lobe, left cerebellum anterior lobe. Regions with SC > HC at fine scales & SC < HC at coarse scales: Inferior FG, occipital, right insula, postcentral gyrus, left middle cingulum.		
[142]	HC 14, AD 15	68 ± 1.6 4, 67 ± 9	400	rest	MSE	m = 2, r = 0.2, scales 1-10	AD: ↓ mean MSE in right hippocampus; functional connectivity ↑ corr. /w MSE at scales 1 and 2 in DMN.		

Reference	Sample	Age (mean ± sd or min - max; TR	Volume	Rest/task	MSE	Method (SE or scales	$m =$ r	Results	
								Parametric	Results
[143]	HC 30, early MCI 33, late MCI 32, AD 29	74 ± 3 6, 72 ± 6, 73 ± 8, 72 ± 7 32, AD 29	140	rest	MSE	$m =$ $2, r$	Generally: HC > MCI > AD; regions with differences include thalamus, insula, lingual gyrus and inferior occipital gyrus, superior FG and olfactory cortex, supramarginal gyrus, superior temporal gyrus, middle temporal gyrus; in regions with differences, cognitive decline corr. /w MSE (varying directions).		
[144]	Adults 14, Children 18	20 ± 2 ?, 9 ± 0.2 18	175	task	MSE	$m =$ $2, r$	Math and grammar tasks: Children < Adults in association cortex.		
[145]	YA 20, middle- aged adults 31, OA 35	23 ± 1.72 3, 54 ± 3, 66 ± 4 = post-encoding; age and memory accuracy ↑ corr. w/ pre-post difference.	175	rest	MSE	$m =$ $2, r$	Memory encoding task: In DMN: for all scales MSE pre-encoding = post-encoding; age and memory accuracy ↑ corr. w/ pre-post difference.		

Reference	Sample	Age (mean ± sd or min - max; TR)	Volume	Rest/task	MSE	Method (SE or		Parameters	Results
[132]	HC 88, MCI 50, AD 7	73 ± 3, 8, 72 ± 7, 67 ± 8 7	197, 420	rest	MSE	$m =$ $2, r$ =	Mean MSE in HC > MCI > AD across whole brain. Tau-PET scales and cognitive impairment ↓ 1-6 corr. /w mean MSE in MTL.		
[146]	ADHD 63, HC 92	10 ± 0.8 1, 10 ± 1	383	rest	MSE	$m =$ $2, r$ =	ADHD: ↓ mean MSE in FPN. Functional connectivity ↑ corr. /w MSE in HC, but not 1-15	ADHD, in FPN and reward and motivation- related circuits.	
[147]	Depression 35, HC 22	68 ± 2 6, 69 ± 6	180	rest	MSE	$m =$ $2, r$ =	Late-life depression: n.s. diff. in mean 0.6, scales	MSE; ↓ scale-1 MSE in right posterior cingulate gyrus; ↑ varying-scale MSE in affective processing (putamen and thalamus), sensory, motor, temporal nodes; ↑ scale-2 MSE in left FPN.	

	Age (mean ± sd or min - max; TR			Method (SE or			Results	
Reference	Sample	years)	(s)	Volume	Rest/task	MSE)	Param.	Results
[148]	504	6-85	1.4	~430	rest, task	MSE	$m =$ $2, r$ $=$ $0.3,$ scales $=$ 1-13	Mean MSE peaks at age 23. Mean MSE ↓ corr. /w 4 of 6 executive function tasks.
[149]	Long scan on YA 5, Short scan YA 8, Short scan OA 8	21 ± 2, 23 ± 2, 66 ± 3	1.37, 2	1000, 240	rest	MSE	$m =$ $2, r$ $=$ $0.3,$ scales $=$ 1-10	MSE in BOLD did not differ from simulated noise. Motion correction ↑ MSE in both gray and white matter. Increasing echo time ↑ MSE in gray matter, but not white matter. MSE ↓ with age.
[150]	53	72- 96	3	120	rest	MSE	$m =$ $1, r$ $=$ 0.35, scales $=$ 1-5	MSE corr. /w ↓ walking speed and ↑ dual-tasks costs.
[151]	Diabetes 10, Dia- betes with- out DPN 10, HC 10	40-DPN2 80		240	rest	MSE	$m =$ $2, r$ $=$ $0.3,$ scales $=$ 1-4	DPN < HC or diabetes without peripheral neuropathy, in basal ganglia.

Reference	Sample	Age (mean ± sd or min - max; TR)	Volume	Rest/task	MSE	Method (SE or	Results	
							Parameter	Results
[152]	PSP MSA	74 ± 2 14, 6, 69 ± 9 18	150	rest	MSE	$m =$ 2, <i>r</i> = 0.3, scales = 1-4	Progressive supranuclear palsy (PSP) < Multiple system atrophy (MSA) in PFC. MSE ↑ corr. /w cognitive function in PFC.	
[153]	28	33 ± 2 8	300	rest	MSE	$m =$ 2, <i>r</i> = 0.3, scales = 1-5	MSE corr. /w various measures of psilocybin level: ↑ at scale 1 (in 7 of 17 networks), n.s. at scales 2-4, ↓ at scale 5 (in 14 of 17 networks).	

	Age (mean ± sd or min - max; TR			Method (SE or			Results
Reference	Sample	years)	(s)	Volume	Rest/task	MSE	Parameter
[154]	20	22- 35	0.72	1200	rest	MSE	$m = 2, r = 0.5, 0.5, 1-25$ Inverted-U pattern of SE across scales. MSE differs from noise (white, pink, red). MSE differs between networks (default mode, cingulo-opercular, left and right frontoparietal). Across networks, MSE \downarrow corr. /w strength and extent of functional connectivity at fine scales but \uparrow corr. at coarse scales.
[155]	Bipolar 125, Schizop- nia 98, Schizoaf- fec- tive	36 ± 12, 18e± 12, 35 ± 13 dis- or- der 107, HC 156	1.5	200	rest	MSE	$m = 1, r = 0.35, 1-5$ Bipolar, schizophrenia, schizoaffective disorder: \downarrow mean scales MSE.

	Age (mean ± sd or min - max; TR			Method (SE or				
	Referen	Sample years)	(s)	Volume	Rest/task	MSE)	Paramet	Results
[156]	20	?	0.72	1200	rest	MSE	$m =$ $2, r$ $=$ $0.5,$ $scales$ $=$ $1-40$	MSE ↓ corr. /w functional connectivity at fine scales, ↑ corr. /w functional connectivity at coarse scales (default mode, left and right executive control, salience networks).
[157]	98	>60	2	180	rest	MSE	$m =$ $1, r$ $=$ $0.5,$ scale $= 5$	Classification of cognitive ability based on MSE in 9 regions.
[158]	Early MCI 87, Late MCI 82, HC 176	73 ± 9, 74 ± 7, 75 ± 9	3	140- 200	rest	MSE	$m =$ $2, r$ $=$ $0.3,$ $scales$ $=$ $1-6$	Early and late MCI: ↓ all-scale MSE (in left fusiform gyrus in early MCI, in rostral ACC in late MCI).

Reference	Sample	Age (mean ± sd or min - max; TR)	Volume	Rest/task	MSE	Method (SE or	Results	
							Parameter	Results
[159]	Schizophrenia 35, 18 HC 30	12 years 2	240	rest	MSE	$m = 1, r = 0.35, \text{scales} = 1-5$	Schizophrenia: ↓ all-scale MSE in left superior parietal lobule and left cuneus; ↑ all-scale MSE in right ventral of middle FG, right superior parietal lobule, right precuneus, bilateral cingulate gyrus.	
[160]	987	22-35	0.72	1200	rest	MSE $m = 2-10, r = 0.15, \text{scales} = 0.5, 1-25$	↑ MSE in DMN and FPNs, ↓ MSE in subcortical areas and limbic system. ↑ MSE at ↓ temporal resolution. Test-retest correlation varies across parameters. Functional brain connectivity corr. /w MSE, direction dependent on scale. Head motion < Resting-state. Intelligence ↑ corr. /w MSE.	

Reference	Sample	Age (mean ± sd or min - max; TR)	Volume	Rest/task	MSE	Method (SE or or)	Parameter	Results
								years)
[161]	YA 100, OA 112	20- 39, 60- 79	2.5	200	rest	MSE	$m =$ $1, r$ $=$ $0.35,$ $scales$ $=$ $1-5?$	In OA but not in YA: APOE 4 allele carriers: ↓ mean MSE in precuneus and posterior cingulate.
[162]	1206	22- 35	0.72	1200	rest	MSE	$m =$ $2, r$ $=$ $0.5,$ $scales$ $=$ $1-12$	Fine-scale MSE ↓ corr. /w surface area, coarse-scale MSE ↑ corr. /w surface area (in lateral frontal and temporal lobes, inferior parietal lobules, and precuneus). Fine-scale MSE ↑ corr. /w cortical myelination, coarse-scale MSE ↓ corr. /w cortical myelination (PFC, lateral temporal lobe, precuneus, lateral parietal cortex, and cingulate cortex).

Reference	Sample	Age (mean ± sd or min - max; TR)	Volume (s)	Rest/task	MSE	$m =$ r	Method (SE or MSE)		Parameters	Results
							Volume	Rest/task	MSE	
[163]	ASD 179, HC 218	16 ± 2 7, 16 ± 6	150- 300	rest	MSE	$m =$ $2, r$ =	ASD: In posterior midline regions, ↑ fine-scale MSE, ↓ coarse-scale MSE; in prefrontal regions, ↓ coarse-scale MSE.			
[164]	Primary 121, Matched repli- ca- tion 122, Non- matched repli- ca- tion 121	28 ± 0.72 3, 28 4, 30 ± 3 1-25	1200	rest	MSE	$m =$ $2, r$ =	White-matter integrity ↑ corr. /w fine-scale MSE and ↓ corr. /w coarse-scale MSE.			
[165]	20000	40- 69?	0.735	490	rest	MSE	$m =$ $2, r$ =	In a predictive model, MSE could predict cognitive phenotypes (fluid intelligence, processing speed, visual memory, and numerical memory), age, and gender moderately well.		

	Age (mean ± sd or min - max; TR			Method (SE or			Param	Results
Reference	Sample	years)	(s)	Volume	Rest/task	MSE		
[166]	100	22- 35	0.72	263- 399	rest, task	MSE	$m = 2, r = 0.5, 1-10$	Tasks can be classified using MSE. Task < 0.5, Rest. Highest MSE in frontoparietal, dorsal attention, visual, and default mode.
[167]	HC 25, MCI 25	70 ± 4, 74 ± 5	2.2, 2.2	164, 164	rest	MSE	$m = 1, r = 0.3, 1-4$	MCI: ↓ scale-2 MSE in R insula, R superior orbitofrontal cortex, and L inferior orbitofrontal cortex.

The entropy-based metrics discussed thus far — Shannon entropy, KS entropy, ApEn, and SE — are maximized with maximum randomness (Figure 11). That is, these metrics are formulated to increase monotonically with series randomness. Contrast this with the definition we described at the beginning, where complexity is a balance of regularity and irregularity, the “ideal” complexity metric should be maximized at an intermediate point between these two extremes. Therefore, strictly speaking, despite being the most commonly used metrics, ApEn and SE do not truly capture “complexity.”

How much of a limitation is this? We are reluctant to dismiss the breadth of good work that has already been completed; in our view, the conflation of complexity and irregularity is only a limitation if, at the scale under investigation, the comparison involves shifts past the midpoint from the domain of irregularity to that of regularity. Although we recognize the limitations of comparing across metrics, we observe that metrics that can describe the full irregularity–regularity range tend to regularity in the adult brain (e.g., avalanche [168]; Hurst [169]; both described later in this review). Therefore, the distinction between complexity and irregularity may be only semantic, at least in the healthy adult brain (but perhaps not in other populations – e.g., infants [170]). Such distinctions could account for the observed inconsistencies across clinical studies, especially

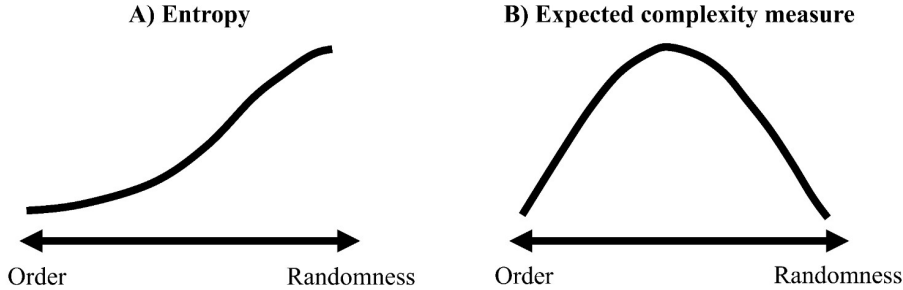


Figure 11: A) Entropy measures (Shannon entropy, SE, ApEn, and others; but not MSE) increase monotonically with data randomness. B) In contrast, an ideal complexity measure would represent the balance between order and disorder. Image adapted from [8]

across neuroimaging modalities (see Discussion). In the next section, we will discuss a method to address this limitation: multiscale sample entropy (MSE).

0.3.5. Multiscale sample entropy

Is a single-scale, like the entropy metrics discussed above, sufficient to describe the brain? The brain is complex across a range of temporal scales, from very short time windows to very long ones, and understanding how these layers interact is essential to understanding the system as a whole [171, 172, 11]. For example, in cross-frequency coupling, high-frequency oscillations (i.e., patterns that recur at fine scales) interact with slow ones, allowing for information transmission [173]. More broadly, fractality — or being similar across multiple scales (discussed below) — appears to be essential to brain function [174]. A better complexity metric would therefore have the ability to describe patterns that occur across multiple scales.

MSE was developed to more fully characterize the complexity of physiological signals by describing SE over multiple scales [175, 138]. This is achieved by downsampling the original time series to multiple lower temporal resolutions to create “new” series across a range of lower frequencies (Figure 12). The SE algorithm is then applied to each series, resulting in a unique SE value for each temporal resolution. That is, the final output consists of a vector of SE values, one for each resolution. Because the output is not a single number, it can be hard to interpret. Typically, results are presented as a plot of SE versus sampling resolution (Figure 13). As an attempt to summarize the output, the slope of this plot or the mean value across scales may also be reported.

Unlike single-scale entropy, MSE can differentiate randomness from complexity. The shape of the scale-MSE curve is neurophysiologically meaningful (Figure 13). MSE for white noise is high at short scales (where there are random fluctuations) and decreases at coarser scales, as fluctuations are smoothed out

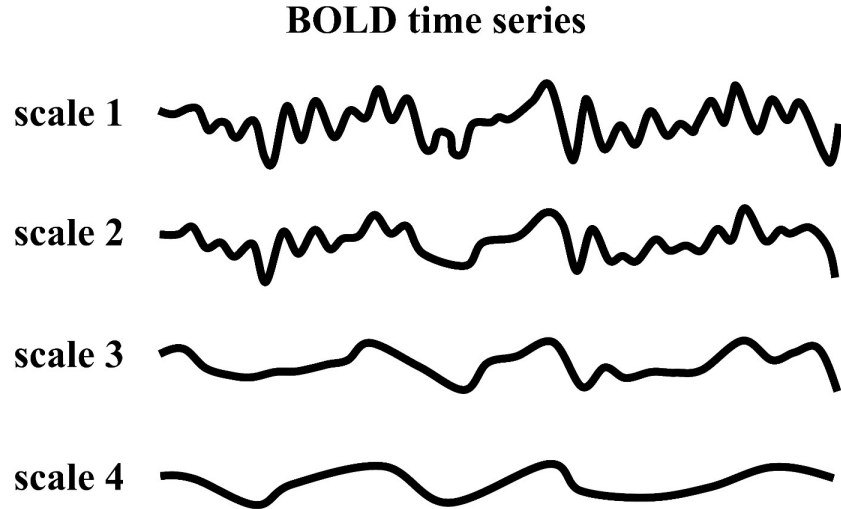


Figure 12: An illustration of downsampling of a time series. Image recreated from [152].

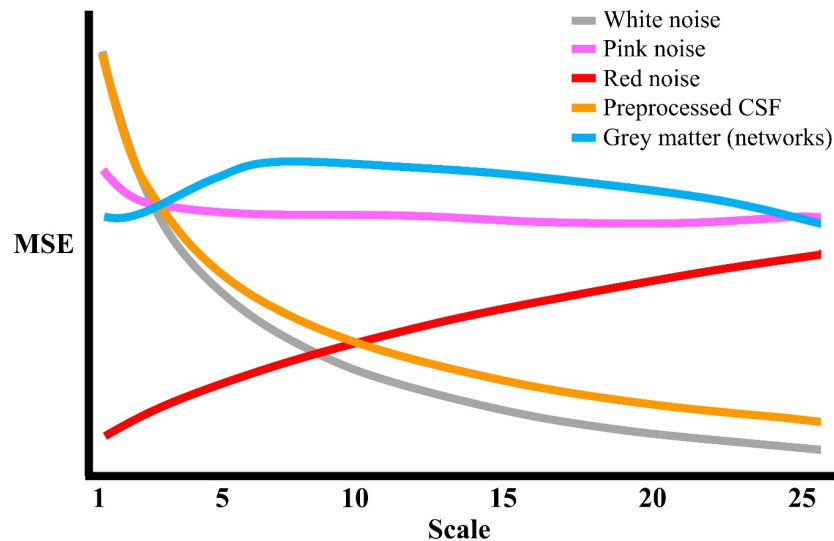


Figure 13: MSE profiles for simulated white, pink, and red noise; preprocessed CSF; and grey matter (resting-state networks). Figure stylized based on results from McDonough et al. (2014). Note that scale is not the same as frequency, as scale and frequency are terms from entirely different frameworks; however, were these concepts to be compared, fine scales (low m values) would roughly map to high frequencies (fast-moving oscillations) and coarse scales (high m) to low frequencies (slow drifts). CSF = cerebrospinal fluid

[[\[154\]](#); hoComplexityAnalysisResting2017] (however, this may be due to bias; see [\[176\]](#)). Fully preprocessed cerebrospinal fluid signal, which in theory consists of a series of uncorrelated random observations and therefore approximates white noise, has a high-then-low MSE curve [\[154\]](#). On the other hand, complex signals, which contain meaningful information across scales, have approximately horizontal MSE curves. For instance, pink and brown noise — which, unlike white noise, contain autocorrelation (i.e., future values are influenced by past ones) — both have characteristic MSE curves (Figure [13](#)), with pink noise, which contains more autocorrelation than brown, having the flatter curve [[\[154\]](#); [\[160\]](#); hoComplexityAnalysisResting2017; smithMultipleTimeScale2014]. Consistent with the idea that BOLD signal from grey matter contains the more meaningful information, its MSE more closely resembles that of pink noise than that of white noise [[\[154\]](#); [\[160\]](#); hoComplexityAnalysisResting2017; smithMultipleTimeScale2014]. See Appendix A2 for an in-depth discussion of the significance of the MSE curve in grey matter, and for a discussion of the major limitations of MSE. See Appendix A3 for detailed instructions on choosing parameters for MSE calculation, including m and r .

What are the limitations of MSE? MSE requires a long time series for proper computation and utilization. Series must be long enough such that the longest scale (e.g., lowest temporal resolution) produced through downsampling contains at least 80 timepoints [\[60\]](#). Furthermore, for MSE to be most useful, the series must be long enough to support multiple resolutions of downsampling. Fortunately for fMRI researchers, [\[12\]](#) showed that MSE can be effectively estimated across discontinuous segments (i.e., multiple runs of fMRI can be concatenated and the estimation will still be effective).

See Table [1](#) for a complete summary of fMRI-MSE studies and their findings.

0.3.6. Other entropy-related measures

Beyond Shannon entropy, ApEn, SE, and MSE, a range of other entropy metrics are available (Figure [14](#)). These metrics are commonly used in other neuroimaging modalities (see [\[6\]](#)), but are seldom employed in fMRI. Table [2](#) summarizes fMRI studies using these metrics.

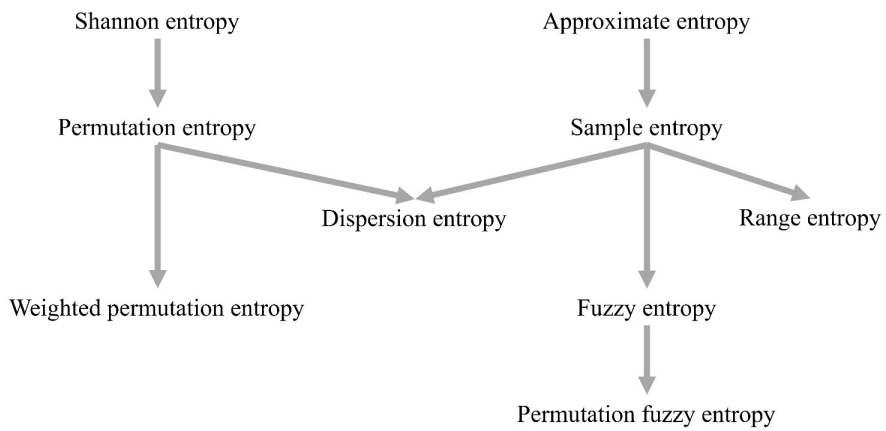


Figure 14: **Historical development of several entropy-related measures used in fMRI time series.** Time proceeds down arrowheads. This is not comprehensive; for instance, RangeEn can be computed using the algorithm for ApEn as well as SE, but only SE is displayed for simplicity. Temporal complexity measures are much more extensively used in EEG/MEG than in fMRI; accordingly, the entropy measures identified in our search represent a small subspace of what is possible. Also, note that nearly all these measures have multiscale versions — e.g., MSE, multiscale permutation entropy, and multiscale fuzzy entropy — are not displayed

Table 2: fMRI studies that use permutation entropy (PE), fuzzy entropy (FuzzyEn), permutation fuzzy entropy (PFE), range entropy (RangeEn), dispersion entropy (DispEn), differential entropy (DiffEn), and Lempel-Ziv complexity (LZC). Studies that use several metrics are not in this table; instead, they are in **?@tbl-comparisons**. HC means healthy controls.

	Sample Reference size	Age (mean \pm sd or min - max; years)	TR (s)	Volumes	Rest/task	Method	Results
[177]	319	6-85	0.645	?	rest	PE	Inverted-U relation- ship be- tween age and PE
[178]	HC 30, early MCI 33, late MCI 32, AD 29	74 \pm 6, 72 \pm 6, 73 \pm 8, 72 \pm 7	3	?	rest	PE	Low PE was associ- ated with Alzheimer's, de- creased cogni- tive func- tion scores, and re- duced grey matter volume

		Age (mean ± sd or min - max; years)	TR (s)	Volumes	Rest/task	Method	Results
[179]	HC 63, Bipolar 48, Schizophre- nia 47, ADHD 40	32 ± 9, 35 ± 9, 36 ± 9, 32 ± 10	2	152	rest	PE	PE can predict risky behaviour in these groups (but was outperformed by measures related to the entropy of FC)
[180]	97	18-30	2.8	134	rest	Multiscale PE	ROI x group (depression vs HC) interaction
[181]	Schizophre- nia 28a± 44, HC 10, 28 30	28a± 10, 28 ± 8	2	190	rest	wPE	wPE is reduced in schizophrenia

		Sample Reference size	Age (mean \pm sd or min - max; years)	TR (s)	Volumes	Rest/task	Method	Results
[182]	Bipolar 49, HC 49	35 \pm 1, 32 \pm 1	2	152	rest	PFE	PFE is altered in bipolar (re- gional in- creases or de- creases)	
[183]	Smokers 11, Non- smokers 13	28 \pm 7, 29 \pm 8	3	255	rest	DispEn	DispEn is lower in non- smokers than in smok- ers	
[181]	998	22-35	0.72	1200	rest	DispEn	DispEn can predict cogni- tive ability and is related to brain anatomy fea- tures	
[71]	50, 130	18-50	2, 2	273, varies	task	LZC	LZC de- creases during all of seven tasks	

		Age (mean ± sd or min - max; years)	TR (s)	Volumes	Rest/task	Method	Results
[184]	1200	22-35	1	varies	task	LZC	LZC decreases during two tasks
[185]	650	18-88	varies	varies	task	LZC	LZC increases during task

0.3.6.1. Permutation entropy.

Permutation entropy (PE) considers only the order of amplitude values, not absolute amplitudes [186]. PE calculation uses a sliding window to slice the series into overlapping segments called “embedded vectors.” Each embedded vector is matched to a motif (called a “permutation pattern” or an “ordinal pattern”), which represents the relative order of the values in the vector. PE is the Shannon entropy of the relative frequencies of the ordinal patterns. That is, PE is closely related to Shannon entropy, but considers the order of values. Compared to ApEn and SE, PE is simpler to compute, makes fewer assumptions, and is more robust in the presence of noise [187].

There are several variants of PE. PE can be computed on downsampled versions of the data (i.e., multiscale permutation entropy), resulting in a description of PE across frequencies [180]. Weighted permutation entropy (wPE) was introduced by [188], and incorporates amplitude information into the PE calculation by multiplying each embedded vector by a weight. Unlike PE, wPE is affected by spikes and abrupt amplitude changes.

0.3.6.2. Fuzzy entropy.

Fuzzy entropy (FuzzyEn) is identical to SE but defines similarity differently [145]. SE defines similarity using the Heaviside function; unfortunately, this function has a rigid boundary, leading to limitations including information loss and parameter-dependence. In contrast, FuzzyEn defines similarity using a fuzzy function and is thus an improved measure of complexity.

0.3.6.3. Permutation fuzzy entropy.

Permutation fuzzy approximate entropy (PFE) was introduced by [85]. It is calculated by first performing permutations on the original time series — which reduces the impact of noise — then computing FuzzyEn. Note that, despite its name, PFE is not directly related to PE.

0.3.6.4. Range entropy.

Range entropy (RangeEn) was introduced to address a limitation of SE and ApEn that is pertinent in EEG, which is that these metrics are not robust to variations in signal amplitude [189]. Compared to SE and ApEn, RangeEn is also less affected by variations in signal length, which makes it an option for short-length fMRI time series [189, 165]. There are two versions of RangeEn: RangeEnA is an improvement to ApEn, and RangeEnB is an improvement to SE [189].

0.3.6.5. Dispersion entropy.

Dispersion entropy (DispEn) originates from SE and PE and corrects a few problems with these respective techniques — namely, that SE is slow to calculate, and that PE does not thoroughly describe changes in amplitude [190]. DispEn is faster to compute than both SE and PE and a better descriptor of frequency and amplitude changes than PE [190].

0.3.6.6. Differential entropy.

Differential entropy (DiffEn) describes the spread of the probability density function for a random variable [191]. It has an interesting history; Claude Shannon thought it was the analogue of discrete entropy for continuous variables, but it is not, and thus is not derived from information-theoretic first principles [191]. Hence, it changes with simple operations to the series like scaling or shifting, and its values are not always meaningful (as they are sometimes negative) [191]. Despite these major limitations, DiffEn has been used in EEG (e.g., [192]); in fMRI, it has been shown to have test-retest reliability comparable to or exceeding those of other temporal complexity metrics [[36]; guanComplexitySpontaneousBrain2023], though no other fMRI studies have used it.

0.4. Lempel-Ziv complexity

0.5. Figures

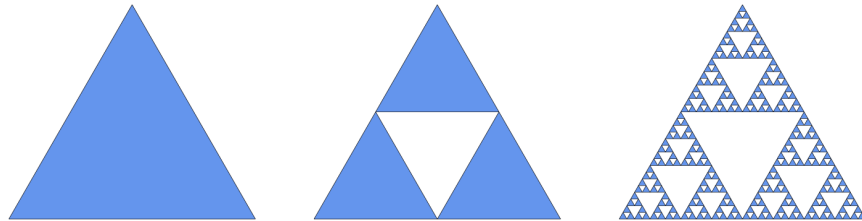
See Figure 15

See Figure 16

See Figure 17

See Figure 18

See Table 3

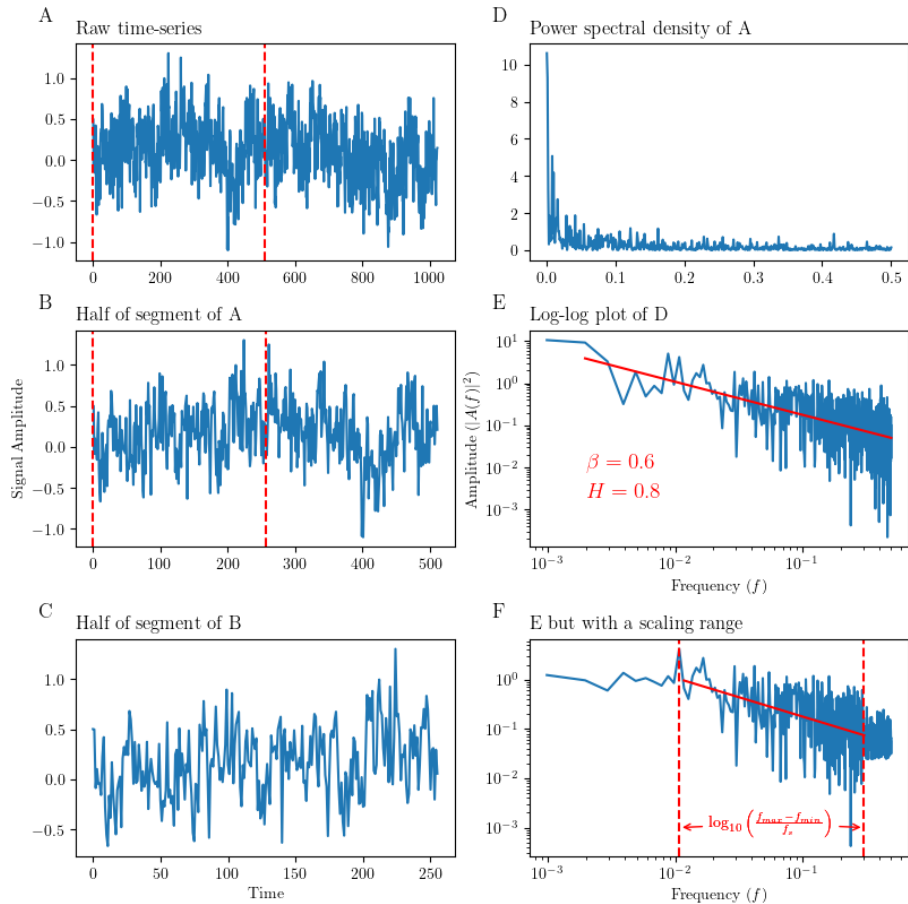


Source: [Figures](#)

Figure 15: Ideal mathematical fractal. The 2D Sierpinski triangle starts with a simple equilateral triangle (left), and subdivides it recursively into smaller equilateral triangles. For every iteration, each triangle (in blue) is further subdivided into four smaller congruent equilateral triangles with the central triangle removed. The first such iteration is shown in the centre, with the fifth iteration shown on the right.

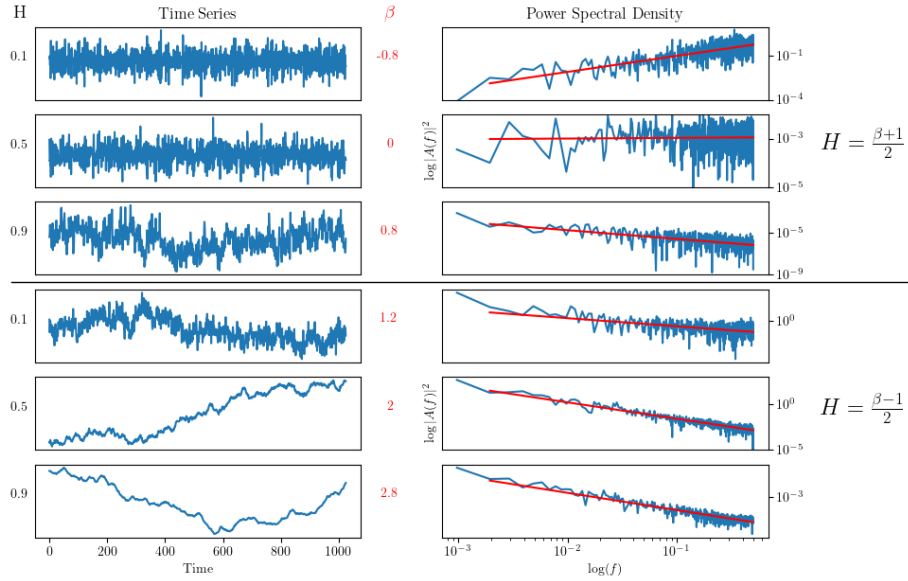


Figure 16: A comparison of statistical and exact fractal patterns. The two basic forms of fractals are demonstrated. Zooming in on tree branches (left), an exact self-similar element cannot be found. Zooming in on an exact fractal (right), exact replica of the whole are found. Photo by author. Branching fractal made in Python. Figure inspired by [193]



Source: [Figures](#)

Figure 17: **Main properties of a fractal time-series** A-C show a raw time-series (fractional Gaussian noise in this example) at different scales: B is the first half of A (shown as vertical dashed lines in A), while C is half of B (shown in vertical dashed lines in B). D is a power spectral density plot of A. E shows D but on a log-log plot, demonstrating the linear nature of fractal signals when plotted on a log-log scale. The slope of E is $-\beta$. In this example, β is calculated to be 0.6, which translates to an H of 0.8. F shows a modified version of E, which imagines that E only demonstrates a power law scaling relationship between two distinct frequencies. The equation for calculating the scaling range in decades is shown. Exact fractal time-series (A) was created using the Davies-Harte method.



Source: [Figures](#)

Figure 18: Simulated fractional Gaussian noise and fractional Brownian motion. Raw simulated time-series with 1,024 time-points and known Hurst values are plotted on the left. The top three time-series are fractional Gaussian noise, while the bottom three are fractional Brownian motion. H values are displayed on the left, while β values are displayed on the right. Note how fractional Gaussian noise remain centered around a mean (i.e. stationary), while fractional Brownian motion wanders away from the mean (i.e. non-stationary). Log-log power spectral density plots of the signals on the left are shown on the right. Linear-regression fits are shown in red, which are used to calculate β and H using the appropriate equation (on the right). Exact fractal time-series were created using the Davies-Harte method. Figure inspired by [194].

Table 3: **fMRI-Hurst studies.** An attempt to gather all published fMRI studies that have used Hurst or Hurst-like analysis, some stats, and the main findings. Main findings are almost certainly more nuanced than how we have reported them here; we have attempted to condense the findings as succinctly as possible. n = number of subjects in the study; TR = repetition time; MLWD = maximum likelihood wavelet; PSD_{Welch} = power spectral density Welch method; DMN = default mode network; DFA = detrended fluctuation analysis; DA = dispersional analysis; SWV = scaled window variance; RS = rescaled range; LW = local Whittle;

Study	n	Age range	Methods	Volumes	TR (s)	Results
[195]	103	19-28	AFA	task: 425, resting: 350	2	impulsivity: ↓
[196]	14	21-29	MLW	2048	1.1	cognitive effort: ↓ H
[169]	72	mean 29	PSD _{Welch}	900	1	movie-watching: ↑ H in visual, somatosensory, and dorsal attention; ↓ frontoparietal and DMN
[197]	97 (28 chemo; 37 radi- ation; 32 HC)	n/a	DFA, Wavelet	285	1.5	worry: ↓ H
[198]	three datasets (98): 19; 49; 30	20-82	DFA, PSD _{Welch}	~ 300	2	age, task novelty and difficulty: ↓ H
[199]	17	18-27	Wavelet	194	2.16	networks
[200]	71 (56 ASD; 15 HC)	mean 13	PSD, DA, SWV	300	2	ASD: ↑ H
[201]	110 (55 mTBI; 55 HC)	mean 13	PSD, DA, SWV	180	2	mTBI: ↑ H
[202]	116	19-85	RS	260	2.5	age: ↑ H frontal and parietal lobe; ↓ H insula, limbic, occipital, temporal lobes

Study	n	Age range	Methods	Volumes	TR (s)	Results
[203]	98	preterm	PSD _{Welch}	100	3	preterm: ↓ H; differentiates networks
[204]	7	21-28	Wavelet	1,000; 1,000, 3,000	1; 0.6; 0.2	microstates
[205]	110	mean 21	PSD, Wavelet	232	2	reappraisal scores: ↓ H
[206]	195 (100; 95)	18-28	Wavelet	?	2	rumination: ↑ H
[207]	31	mean 25	Wavelet	512	1.64	neuroticism: ↓
[208]	36	mean 27	Wavelet	450	2	social anxiety: ↑ H
[21]	17	18-27	DFA, PSD	194	2.16	task: ↓ H; differentiates networks; brain glucose metabolism and neurovascular coupling
[209]	40 (20 task; 20 no task)	20-32	DFA	512	1.13	motor sequence learning: ↓ H
[210]	63 (33 ASD; 3- HC)	n/a	Wavelet	512	1.3	ASD: ↓ H
[211]	17	18-29	Wavelet	200	1.5	extroversion: ↓ H in DMN
[212]	75 (16 HMMD; 34 IMMD; 25 HC)	mean ~ 41	RS	240	2	moyamoya disease: ↓ H
[213]	83	1.5-5	WML	400	0.8	age of children ASD: ↓ H in vmPFC
[214]	21	n/a	LW, Wor- nell, MLW	150	2	AD: ↑ H

Study	n	Age range	Methods	Volumes	TR (s)	Results
[170]	716	preterm	PSD _{Welch}	2,300	0.392	preterm: ↓ H; H starts < 0.5 at preterm age ; differentiates networks
[215]	100	22-35	PSD, DFA	min 250	0.72	cognitive load: ↓ H; H and entropy-based complexity highly correlated; H highest in frontoparietal network and default mode network
[216]	22	?	Many	?	?	HFFT and PSD _{Welch} outperform other methods
[122]	29 (13 SZ; 16 HC)	?	DA, DFA	?	?	SZ: ↓ H
[217]	22 (11 old; 11 young)	22 and 65	MLW	512	1.1	multifractal reanalysis of [218]
[219]	23	mean 23.9	DFA	300	2	fear: ↓ H then ↑ H
[220]	124 (55 TD; 30 AT; 39 SZ)	?	Wavelet	947?	0.475	ASD and SZ: ↓ H
[221]	33 (15 HC; 10 min con- scious; 8 veg)	?	HFD	?	?	Lower consciousness: ↓ H

Study	n	Age range	Methods	Volumes	TR (s)	Results
[46]	?	?	Wavelet, DFA	1500	2.08	multiscale variance effects produce Hurst phenomena without long-range dependence
[222]	46 (33 AD; 13 HC)	?	PSD, RD	2,400	0.25	AD: ↑ H
[223]	14	22-38	Wavelet	512	2	acute alcohol intoxication: mix of <i>uparrow</i> and <i>downarrow</i> H
[218]	22 (11 old; 11 young)	22 and 65	MLW	512	1.1	age: ↑ H in bilateral hippocampus; scopolamine: ↑ H; faster task: ↑ H
[224]	11	mean 35 ± 10	Wavelet	136	1.1	latency in fame decision task: ↓ H
[225]	70	?	Wavelet	700	0.6	pharmacoresistant TLE: ↓ H

References

- [1] T. F. Varley, A. I. Luppi, I. Pappas, L. Naci, R. Adapa, A. M. Owen, D. K. Menon, E. A. Stamatakis, Consciousness & Brain Functional Complexity in Propofol Anaesthesia, *Scientific Reports* 10 (1) (2020) 1018. [doi:10.1038/s41598-020-57695-3](https://doi.org/10.1038/s41598-020-57695-3).
- [2] J. Sun, B. Wang, Y. Niu, Y. Tan, C. Fan, N. Zhang, J. Xue, J. Wei, J. Xiang, J. Sun, B. Wang, Y. Niu, Y. Tan, C. Fan, N. Zhang, J. Xue, J. Wei, J. Xiang, Complexity Analysis of EEG, MEG, and fMRI in Mild Cognitive Impairment and Alzheimer's Disease: A Review, *Entropy* 22 (2) (Feb. 2020). [doi:10.3390/e22020239](https://doi.org/10.3390/e22020239).
- [3] R. Cofré, A. Destexhe, R. Cofré, A. Destexhe, Entropy and Complexity Tools Across Scales in Neuroscience: A Review, *Entropy* 27 (2) (Jan. 2025). [doi:10.3390/e27020115](https://doi.org/10.3390/e27020115).

- [4] S. Sarasso, A. G. Casali, S. Casarotto, M. Rosanova, C. Sinigaglia, M. Massimini, Consciousness and complexity: A consilience of evidence, *Neuroscience of Consciousness* 2021 (2) (2021) niab023. [doi:10.1093/nc/niab023](https://doi.org/10.1093/nc/niab023).
- [5] R. M. Hernández, J. C. Ponce-Meza, M. Á. Saavedra-López, W. A. Campos Ugaz, R. M. Chanduvi, W. C. Monteza, Brain Complexity and Psychiatric Disorders, *Iranian Journal of Psychiatry* (Sep. 2023). [doi:10.18502/ijps.v18i4.13637](https://doi.org/10.18502/ijps.v18i4.13637).
- [6] S. Keshmiri, Entropy and the Brain: An Overview, *Entropy* 22 (9) (2020) 917. [doi:10.3390/e22090917](https://doi.org/10.3390/e22090917).
- [7] T. Donoghue, R. Hammonds, E. Lybrand, L. Washcke, R. Gao, B. Voytek, Evaluating and Comparing Measures of Aperiodic Neural Activity (Sep. 2024). [doi:10.1101/2024.09.15.613114](https://doi.org/10.1101/2024.09.15.613114).
- [8] A. C. Yang, S.-J. Tsai, Is mental illness complex? From behavior to brain, *Progress in Neuro-Psychopharmacology and Biological Psychiatry* 45 (2013) 253–257. [doi:10.1016/j.pnpbp.2012.09.015](https://doi.org/10.1016/j.pnpbp.2012.09.015).
- [9] T. Ros, B. J. Baars, R. A. Lanius, P. Vuilleumier, Tuning pathological brain oscillations with neurofeedback: A systems neuroscience framework, *Frontiers in Human Neuroscience* 8 (Dec. 2014). [doi:10.3389/fnhum.2014.01008](https://doi.org/10.3389/fnhum.2014.01008).
- [10] I. Cifre, M. Zarepour, S. G. Horovitz, S. A. Cannas, D. R. Chialvo, Further results on why a point process is effective for estimating correlation between brain regions, *Papers in Physics* 12 (2020) 120003. [doi:10.4279/pip.120003](https://doi.org/10.4279/pip.120003).
- [11] R. F. Betzel, D. S. Bassett, Multi-scale brain networks, *NeuroImage* 160 (2017) 73–83. [doi:10.1016/j.neuroimage.2016.11.006](https://doi.org/10.1016/j.neuroimage.2016.11.006).
- [12] T. H. Grandy, D. D. Garrett, F. Schmiedek, M. Werkle-Bergner, On the estimation of brain signal entropy from sparse neuroimaging data, *Scientific Reports* 6 (1) (2016) 23073. [doi:10.1038/srep23073](https://doi.org/10.1038/srep23073).
- [13] M. O. Sokunbi, BOLD fMRI complexity predicts changes in brain processes, interactions and patterns, in health and disease, *Journal of the Neurological Sciences* 367 (2016) 347–348. [doi:10.1016/j.jns.2016.06.040](https://doi.org/10.1016/j.jns.2016.06.040).
- [14] X. Xin, S. Long, M. Sun, X. Gao, X. Xin, S. Long, M. Sun, X. Gao, The Application of Complexity Analysis in Brain Blood-Oxygen Signal, *Brain Sciences* 11 (11) (Oct. 2021). [doi:10.3390/brainsci11111415](https://doi.org/10.3390/brainsci11111415).
- [15] O. Sporns, Networks of the Brain, The MIT Press, 2010. [doi:10.7551/mitpress/8476.001.0001](https://doi.org/10.7551/mitpress/8476.001.0001).

- [16] J. S. Richman, J. R. Moorman, Physiological time-series analysis using approximate entropy and sample entropy, *American Journal of Physiology-Heart and Circulatory Physiology* 278 (6) (2000) H2039–H2049. [doi:10.1152/ajpheart.2000.278.6.H2039](https://doi.org/10.1152/ajpheart.2000.278.6.H2039).
- [17] H. E. Hurst, Long-Term Storage Capacity of Reservoirs, *Transactions of the American Society of Civil Engineers* 116 (1) (1951) 770–799. [doi:10.1061/TACEAT.0006518](https://doi.org/10.1061/TACEAT.0006518).
- [18] N. Lotfi, T. Feliciano, L. A. A. Aguiar, T. P. L. Silva, T. T. A. Carvalho, O. A. Rosso, M. Copelli, F. S. Matias, P. V. Carelli, Statistical complexity is maximized close to criticality in cortical dynamics, *Physical Review E* 103 (1) (2021) 012415. [doi:10.1103/PhysRevE.103.012415](https://doi.org/10.1103/PhysRevE.103.012415).
- [19] D. D. Garrett, G. R. Samanez-Larkin, S. W. MacDonald, U. Lindenberger, A. R. McIntosh, C. L. Grady, Moment-to-moment brain signal variability: A next frontier in human brain mapping?, *Neuroscience & Biobehavioral Reviews* 37 (4) (2013) 610–624. [doi:10.1016/j.neubiorev.2013.02.015](https://doi.org/10.1016/j.neubiorev.2013.02.015).
- [20] D. Chialvo, Life at the Edge: Complexity and Criticality in Biological Function, *Acta Physica Polonica B* 49 (12) (2018) 1955. [doi:10.5506/APhysPolB.49.1955](https://doi.org/10.5506/APhysPolB.49.1955).
- [21] B. J. He, Scale-Free Properties of the Functional Magnetic Resonance Imaging Signal during Rest and Task, *The Journal of Neuroscience* 31 (39) (2011) 13786–13795. [doi:10.1523/JNEUROSCI.2111-11.2011](https://doi.org/10.1523/JNEUROSCI.2111-11.2011).
- [22] B. Li, P.-l. Zhang, Z.-j. Wang, S.-s. Mi, P.-y. Liu, Morphological covering based generalized dimension for gear fault diagnosis, *Nonlinear Dynamics* 67 (4) (2012) 2561–2571. [doi:10.1007/s11071-011-0169-1](https://doi.org/10.1007/s11071-011-0169-1).
- [23] D. D. Garrett, N. Kovacevic, A. R. McIntosh, C. L. Grady, Blood Oxygen Level-Dependent Signal Variability Is More than Just Noise, *The Journal of Neuroscience* 30 (14) (2010) 4914–4921. [doi:10.1523/JNEUROSCI.5166-09.2010](https://doi.org/10.1523/JNEUROSCI.5166-09.2010).
- [24] C. Shannon, Communication in the Presence of Noise, *Proceedings of the IRE* 37 (1) (1949) 10–21. [doi:10.1109/JRPROC.1949.232969](https://doi.org/10.1109/JRPROC.1949.232969).
- [25] L. Serrano, Shannon Entropy, Information Gain, and Picking Balls from Buckets (Oct. 2018).
- [26] A. Viol, F. Palhano-Fontes, H. Onias, D. B. de Araujo, G. M. Viswanathan, Shannon entropy of brain functional complex networks under the influence of the psychedelic Ayahuasca, *Scientific Reports* 7 (1) (2017) 7388. [doi:10.1038/s41598-017-06854-0](https://doi.org/10.1038/s41598-017-06854-0).

- [27] I. Pappas, R. M. Adapa, D. K. Menon, E. A. Stamatakis, Brain network disintegration during sedation is mediated by the complexity of sparsely connected regions, *NeuroImage* 186 (2019) 221–233. [doi:10.1016/j.neuroimage.2018.10.078](https://doi.org/10.1016/j.neuroimage.2018.10.078).
- [28] H. Huang, X. Qin, R. Xu, Y. Xiong, K. Hao, C. Chen, Q. Wan, H. Liu, W. Yuan, Y. Peng, Y. Zhou, H. Wang, L. Palaniyappan, Default Mode Network, Disorganization, and Treatment-Resistant Schizophrenia, *Schizophrenia Bulletin* (2025) sbaf018[doi:10.1093/schbul/sbaf018](https://doi.org/10.1093/schbul/sbaf018).
- [29] O. A. Rosso, S. Blanco, J. Yordanova, V. Kolev, A. Figliola, M. Schürmann, E. Başar, Wavelet entropy: A new tool for analysis of short duration brain electrical signals, *Journal of Neuroscience Methods* 105 (1) (2001) 65–75. [doi:10.1016/S0165-0270\(00\)00356-3](https://doi.org/10.1016/S0165-0270(00)00356-3).
- [30] L. Gupta, J. F. Jansen, P. A. Hofman, R. M. Besseling, A. J. De Louw, A. P. Aldenkamp, W. H. Backes, Wavelet entropy of BOLD time series: An application to Rolandic epilepsy, *Journal of Magnetic Resonance Imaging* 46 (6) (2017) 1728–1737. [doi:10.1002/jmri.25700](https://doi.org/10.1002/jmri.25700).
- [31] P. Mikoláš, J. Vyhnanek, A. Škoch, J. Horáček, Analysis of fMRI time-series by entropy measures, *Neuro Endocrinology Letters* 33 (5) (2012) 471–476.
- [32] D. Ostwald, A. P. Bagshaw, Information theoretic approaches to functional neuroimaging, *Magnetic Resonance Imaging* 29 (10) (2011) 1417–1428. [doi:10.1016/j.mri.2011.07.013](https://doi.org/10.1016/j.mri.2011.07.013).
- [33] D. De Araujo, W. Tedeschi, A. Santos, J. Elias, U. Neves, O. Baffa, Shannon entropy applied to the analysis of event-related fMRI time series, *NeuroImage* 20 (1) (2003) 311–317. [doi:10.1016/S1053-8119\(03\)00306-9](https://doi.org/10.1016/S1053-8119(03)00306-9).
- [34] M. DiNuzzo, D. Mascali, M. Moraschi, G. Bussu, B. Maraviglia, S. Mangia, F. Giove, Temporal Information Entropy of the Blood-Oxygenation Level-Dependent Signals Increases in the Activated Human Primary Visual Cortex, *Frontiers in Physics* 5 (Feb. 2017). [doi:10.3389/fphy.2017.00007](https://doi.org/10.3389/fphy.2017.00007).
- [35] M. J. Sturzbecher, W. Tedeschi, B. C. T. Cabella, O. Baffa, U. P. C. Neves, D. B. De Araujo, Non-extensive entropy and the extraction of BOLD spatial information in event-related functional MRI, *Physics in Medicine and Biology* 54 (1) (2009) 161–174. [doi:10.1088/0031-9155/54/1/011](https://doi.org/10.1088/0031-9155/54/1/011).
- [36] X. Wang, Y. Jiao, T. Tang, H. Wang, Z. Lu, Investigating univariate temporal patterns for intrinsic connectivity networks based on complexity and low-frequency oscillation: A test-retest reliability study, *Neuroscience* 254 (2013) 404–426. [doi:10.1016/j.neuroscience.2013.09.009](https://doi.org/10.1016/j.neuroscience.2013.09.009).
- [37] S. Gonzalez Andino, R. Grave de Peralta Menendez, G. Thut, L. Spinelli, O. Blanke, C. Michel, T. Landis, Measuring the complexity of time series:

- An application to neurophysiological signals, *Human Brain Mapping* 11 (1) (2000) 46–57. [doi:10.1002/1097-0193\(200009\)11:1<46::AID-HBM40>3.0.CO;2-5](https://doi.org/10.1002/1097-0193(200009)11:1<46::AID-HBM40>3.0.CO;2-5).
- [38] B. C. Cabella, M. J. Sturzbecher, D. B. De Araujo, U. P. Neves, Generalized relative entropy in functional magnetic resonance imaging, *Physica A: Statistical Mechanics and its Applications* 388 (1) (2009) 41–50. [doi:10.1016/j.physa.2008.09.029](https://doi.org/10.1016/j.physa.2008.09.029).
 - [39] M. Welvaert, Y. Rosseel, How ignoring physiological noise can bias the conclusions from fMRI simulation results, *Journal of Neuroscience Methods* 211 (1) (2012) 125–132. [doi:10.1016/j.jneumeth.2012.08.022](https://doi.org/10.1016/j.jneumeth.2012.08.022).
 - [40] J. W. Fisher, E. R. Cosman, C. Wible, W. M. Wells, Adaptive Entropy Rates for fMRI Time-Series Analysis, in: G. Goos, J. Hartmanis, J. Van Leeuwen, W. J. Niessen, M. A. Viergever (Eds.), *Medical Image Computing and Computer-Assisted Intervention – MICCAI 2001*, Vol. 2208, Springer Berlin Heidelberg, Berlin, Heidelberg, 2001, pp. 905–912. [doi:10.1007/3-540-45468-3_108](https://doi.org/10.1007/3-540-45468-3_108).
 - [41] A. Tsai, J. W. Fisher, C. Wible, W. M. Wells, J. Kim, A. S. Willsky, Analysis of Functional MRI Data Using Mutual Information, in: G. Goos, J. Hartmanis, J. Van Leeuwen, C. Taylor, A. Colchester (Eds.), *Medical Image Computing and Computer-Assisted Intervention – MICCAI'99*, Vol. 1679, Springer Berlin Heidelberg, Berlin, Heidelberg, 1999, pp. 473–480. [doi:10.1007/10704282_51](https://doi.org/10.1007/10704282_51).
 - [42] G. Fuhrmann Alpert, F. T. Sun, D. Handwerker, M. D’Esposito, R. T. Knight, Spatio-temporal information analysis of event-related BOLD responses, *NeuroImage* 34 (4) (2007) 1545–1561. [doi:10.1016/j.neuroimage.2006.10.020](https://doi.org/10.1016/j.neuroimage.2006.10.020).
 - [43] G. F. Alpert, G. Hein, N. Tsai, M. J. Naumer, R. T. Knight, Temporal Characteristics of Audiovisual Information Processing, *The Journal of Neuroscience* 28 (20) (2008) 5344–5349. [doi:10.1523/JNEUROSCI.5039-07.2008](https://doi.org/10.1523/JNEUROSCI.5039-07.2008).
 - [44] W. Tedeschi, H.-P. Müller, D. De Araujo, A. Santos, U. Neves, S. Erné, O. Baffa, Generalized mutual information fMRI analysis: A study of the Tsallis q parameter, *Physica A: Statistical Mechanics and its Applications* 344 (3-4) (2004) 705–711. [doi:10.1016/j.physa.2004.06.052](https://doi.org/10.1016/j.physa.2004.06.052).
 - [45] W. Tedeschi, H.-P. Müller, D. De Araujo, A. Santos, U. Neves, S. Erné, O. Baffa, Generalized mutual information tests applied to fMRI analysis, *Physica A: Statistical Mechanics and its Applications* 352 (2-4) (2005) 629–644. [doi:10.1016/j.physa.2004.12.065](https://doi.org/10.1016/j.physa.2004.12.065).
 - [46] F. Von Wegner, H. Laufs, E. Tagliazucchi, Mutual information identifies spurious Hurst phenomena in resting state EEG and fMRI data, *Physical Review E* 97 (2) (2018) 022415. [doi:10.1103/PhysRevE.97.022415](https://doi.org/10.1103/PhysRevE.97.022415).

- [47] P. Metzak, E. Feredoes, Y. Takane, L. Wang, S. Weinstein, T. Cairo, E. T. Ngan, T. S. Woodward, Constrained principal component analysis reveals functionally connected load-dependent networks involved in multiple stages of working memory, *Human Brain Mapping* 32 (6) (2011) 856–871. [doi:10.1002/hbm.21072](https://doi.org/10.1002/hbm.21072).
- [48] M. Nogueira, Exploring the link between multiscale entropy and fractal scaling behavior in near-surface wind, *PLOS ONE* 12 (3) (2017) e0173994. [doi:10.1371/journal.pone.0173994](https://doi.org/10.1371/journal.pone.0173994).
- [49] S. M. Pincus, Approximate entropy as a measure of system complexity., *Proceedings of the National Academy of Sciences* 88 (6) (1991) 2297–2301. [doi:10.1073/pnas.88.6.2297](https://doi.org/10.1073/pnas.88.6.2297).
- [50] J. Bruhn, H. Röpcke, A. Hoeft, Approximate Entropy as an Electroencephalographic Measure of Anesthetic Drug Effect during Desflurane Anesthesia, *Anesthesiology* 92 (3) (2000) 715–726. [doi:10.1097/00000542-200003000-00016](https://doi.org/10.1097/00000542-200003000-00016).
- [51] M. O. Sokunbi, R. T. Staff, G. D. Waiter, T. S. Ahearn, H. C. Fox, I. J. Deary, J. M. Starr, L. J. Whalley, A. D. Murray, Inter-individual Differences in fMRI Entropy Measurements in Old Age, *IEEE Transactions on Biomedical Engineering* 58 (11) (2011) 3206–3214. [doi:10.1109/TBME.2011.2164793](https://doi.org/10.1109/TBME.2011.2164793).
- [52] C. Y. Liu, A. P. Krishnan, L. Yan, R. X. Smith, E. Kilroy, J. R. Alger, J. M. Ringman, D. J. Wang, Complexity and synchronicity of resting state blood oxygenation level-dependent (BOLD) functional MRI in normal aging and cognitive decline: Complexity of BOLD fMRI in Aging, *Journal of Magnetic Resonance Imaging* 38 (1) (2013) 36–45. [doi:10.1002/jmri.23961](https://doi.org/10.1002/jmri.23961).
- [53] A. C. Yang, S.-J. Tsai, C.-P. Lin, C.-K. Peng, A Strategy to Reduce Bias of Entropy Estimates in Resting-State fMRI Signals, *Frontiers in Neuroscience* 12 (2018) 398. [doi:10.3389/fnins.2018.00398](https://doi.org/10.3389/fnins.2018.00398).
- [54] Z. Wang, Y. Li, A. R. Childress, J. A. Detre, Brain Entropy Mapping Using fMRI, *PLOS ONE* 9 (3) (2014) e89948. [doi:10.1371/journal.pone.0089948](https://doi.org/10.1371/journal.pone.0089948).
- [55] N. Zhang, Y. Niu, J. Sun, W. An, D. Li, J. Wei, T. Yan, J. Xiang, B. Wang, Altered Complexity of Spontaneous Brain Activity in Schizophrenia and Bipolar Disorder Patients, *Journal of Magnetic Resonance Imaging* 54 (2) (2021) 586–595. [doi:10.1002/jmri.27541](https://doi.org/10.1002/jmri.27541).
- [56] G. Akdeniz, Complexity Analysis of Resting-State fMRI in Adult Patients with Attention Deficit Hyperactivity Disorder: Brain Entropy, *Computational Intelligence and Neuroscience* 2017 (2017) 1–6. [doi:10.1155/2017/3091815](https://doi.org/10.1155/2017/3091815).

- [57] A. Delgado-Bonal, A. Marshak, Approximate Entropy and Sample Entropy: A Comprehensive Tutorial, *Entropy* 21 (6) (2019) 541. [doi:10.3390/e21060541](https://doi.org/10.3390/e21060541).
- [58] D. J. Roediger, J. Butts, C. Falke, M. B. Fiecas, B. Klimes-Dougan, B. A. Mueller, K. R. Cullen, Optimizing the measurement of sample entropy in resting-state fMRI data, *Frontiers in Neurology* 15 (Feb. 2024). [doi:10.3389/fneur.2024.1331365](https://doi.org/10.3389/fneur.2024.1331365).
- [59] M. H. Wehrheim, J. Faskowitz, A.-L. Schubert, C. J. Fiebach, Reliability of variability and complexity measures for task and task-free BOLD fMRI, *Human Brain Mapping* 45 (10) (2024) e26778. [doi:10.1002/hbm.26778](https://doi.org/10.1002/hbm.26778).
- [60] M. O. Sokunbi, Sample entropy reveals high discriminative power between young and elderly adults in short fMRI data sets, *Frontiers in Neuroinformatics* 8 (Jul. 2014). [doi:10.3389/fninf.2014.00069](https://doi.org/10.3389/fninf.2014.00069).
- [61] G. Del Mauro, Z. Wang, Cross-subject brain entropy mapping (Apr. 2024). [doi:10.1101/2024.04.05.588307](https://doi.org/10.1101/2024.04.05.588307).
- [62] Z. Wang, The neurocognitive correlates of brain entropy estimated by resting state fMRI, *NeuroImage* 232 (2021) 117893. [doi:10.1016/j.neuroimage.2021.117893](https://doi.org/10.1016/j.neuroimage.2021.117893).
- [63] J. O. Maximo, C. M. Nelson, R. K. Kana, “Unrest while Resting”? Brain entropy in autism spectrum disorder, *Brain Research* 1762 (2021) 147435. [doi:10.1016/j.brainres.2021.147435](https://doi.org/10.1016/j.brainres.2021.147435).
- [64] Z. Wang, J. Suh, D. Duan, S. Darnley, Y. Jing, J. Zhang, C. O’Brien, A. R. Childress, A hypo-status in drug-dependent brain revealed by multimodal MRI, *Addiction Biology* 22 (6) (2017) 1622–1631. [doi:10.1111/adb.12459](https://doi.org/10.1111/adb.12459).
- [65] S. Fu, X. Wang, Z. Chen, Z. Huang, Y. Feng, Y. Xie, X. Li, C. Yang, S. Xu, Abnormalities in Brain Complexity in Children with Autism Spectrum Disorder: A Sleeping State Functional MRI Study. (Oct. 2024). [doi:10.21203/rs.3.rs-4966735/v1](https://doi.org/10.21203/rs.3.rs-4966735/v1).
- [66] L. Sevel, B. Stennett, V. Schneider, N. Bush, S. J. Nixon, M. Robinson, J. Boissoneault, Acute Alcohol Intake Produces Widespread Decreases in Cortical Resting Signal Variability in Healthy Social Drinkers, *Alcoholism: Clinical and Experimental Research* 44 (7) (2020) 1410–1419. [doi:10.1111/acer.14381](https://doi.org/10.1111/acer.14381).
- [67] D. Song, Z. Wang, Age-dependent effects of intranasal oxytocin administration were revealed by resting brain entropy (BEN) (Nov. 2024). [doi:10.1101/2024.11.25.625152](https://doi.org/10.1101/2024.11.25.625152).

- [68] Z. Zhao, Y. Shuai, Y. Wu, X. Xu, M. Li, D. Wu, Age-dependent functional development pattern in neonatal brain: An fMRI-based brain entropy study, *NeuroImage* 297 (2024) 120669. [doi:10.1016/j.neuroimage.2024.120669](https://doi.org/10.1016/j.neuroimage.2024.120669).
- [69] X. Jiang, X. Li, H. Xing, X. Huang, X. Xu, J. Li, Brain Entropy Study on Obsessive-Compulsive Disorder Using Resting-State fMRI, *Frontiers in Psychiatry* 12 (2021) 764328. [doi:10.3389/fpsyg.2021.764328](https://doi.org/10.3389/fpsyg.2021.764328).
- [70] B. Sharma, C. Nowikow, C. Zhu, M. D. Noseworthy, Which voxel-wise resting state fMRI metric is the most discriminatory for concussion? A secondary analysis. (Jul. 2024). [doi:10.21203/rs.3.rs-4578572/v1](https://doi.org/10.21203/rs.3.rs-4578572/v1).
- [71] Y. Çatal, M. A. Günay, C. Li, J. Wang, H. Cui, W. Li, G. Northoff, The Intrinsic Hierarchy of Self – Converging Topography and Dynamics (Jun. 2022). [doi:10.1101/2022.06.23.497287](https://doi.org/10.1101/2022.06.23.497287).
- [72] X. Liu, D. Song, Y. Yin, C. Xie, H. Zhang, H. Zhang, Z. Zhang, Z. Wang, Y. Yuan, Altered Brain Entropy as a predictor of antidepressant response in major depressive disorder, *Journal of Affective Disorders* 260 (2020) 716–721. [doi:10.1016/j.jad.2019.09.067](https://doi.org/10.1016/j.jad.2019.09.067).
- [73] D. Song, D. Chang, J. Zhang, Q. Ge, Y.-F. Zang, Z. Wang, Associations of brain entropy (BEN) to cerebral blood flow and fractional amplitude of low-frequency fluctuations in the resting brain, *Brain Imaging and Behavior* 13 (5) (2019) 1486–1495. [doi:10.1007/s11682-018-9963-4](https://doi.org/10.1007/s11682-018-9963-4).
- [74] G. Del Mauro, Z. Wang, Associations of Brain Entropy Estimated by Resting State fMRI With Physiological Indices, Body Mass Index, and Cognition, *Journal of Magnetic Resonance Imaging* 59 (5) (2024) 1697–1707. [doi:10.1002/jmri.28948](https://doi.org/10.1002/jmri.28948).
- [75] A. K. Easson, A. R. McIntosh, BOLD signal variability and complexity in children and adolescents with and without autism spectrum disorder, *Developmental Cognitive Neuroscience* 36 (2019) 100630. [doi:10.1016/j.dcn.2019.100630](https://doi.org/10.1016/j.dcn.2019.100630).
- [76] G. N. Saxe, D. Calderone, L. J. Morales, Brain entropy and human intelligence: A resting-state fMRI study, *PLOS ONE* 13 (2) (2018) e0191582. [doi:10.1371/journal.pone.0191582](https://doi.org/10.1371/journal.pone.0191582).
- [77] X. Liu, X. Ge, X. Tang, H. Ye, L. Pan, X. Zhu, H. Hu, Z. Ding, L. Wang, Brain entropy changes in classical trigeminal neuralgia, *Frontiers in Neurology* 14 (2023) 1273336. [doi:10.3389/fneur.2023.1273336](https://doi.org/10.3389/fneur.2023.1273336).
- [78] L. Shi, R. E. Beaty, Q. Chen, J. Sun, D. Wei, W. Yang, J. Qiu, Brain Entropy is Associated with Divergent Thinking, *Cerebral Cortex* (2019) bhz120 [doi:10.1093/cercor/bhz120](https://doi.org/10.1093/cercor/bhz120).

- [79] Z. Wang, for the Alzheimer's Disease Neuroimaging Initiative, Brain Entropy Mapping in Healthy Aging and Alzheimer's Disease, *Frontiers in Aging Neuroscience* 12 (2020) 596122. [doi:10.3389/fnagi.2020.596122](https://doi.org/10.3389/fnagi.2020.596122).
- [80] Z. Y. Shan, K. Finegan, S. Bhuta, T. Ireland, D. R. Staines, S. M. Marshall-Gradisnik, L. R. Barnden, Brain function characteristics of chronic fatigue syndrome: A task fMRI study, *NeuroImage: Clinical* 19 (2018) 279–286. [doi:10.1016/j.nicl.2018.04.025](https://doi.org/10.1016/j.nicl.2018.04.025).
- [81] J. B. Allendorfer, R. Nenert, A. M. Goodman, P. Kakulamarri, S. Correia, N. S. Philip, W. C. LaFrance, J. P. Szaflarski, Brain network entropy, depression, and quality of life in people with traumatic brain injury and seizure disorders, *Epilepsia Open* 9 (3) (2024) 969–980. [doi:10.1002/epi4.12926](https://doi.org/10.1002/epi4.12926).
- [82] D. Chang, D. Song, J. Zhang, Y. Shang, Q. Ge, Z. Wang, Caffeine Caused a Widespread Increase of Resting Brain Entropy, *Scientific Reports* 8 (1) (2018) 2700. [doi:10.1038/s41598-018-21008-6](https://doi.org/10.1038/s41598-018-21008-6).
- [83] Mackenzie Joel Leavitt, Characterizing Brain Entropy During a Face-Name Paired Association Task, Master's thesis, Auburn University (Aug. 2022).
- [84] W. Jiang, L. Cai, Z. Wang, Common hyper-entropy patterns identified in nicotine smoking, marijuana use, and alcohol use based on uni-drug dependence cohorts, *Medical & Biological Engineering & Computing* 61 (12) (2023) 3159–3166. [doi:10.1007/s11517-023-02932-w](https://doi.org/10.1007/s11517-023-02932-w).
- [85] Y. Niu, J. Sun, B. Wang, W. Hussain, C. Fan, R. Cao, M. Zhou, J. Xiang, Comparing Test-Retest Reliability of Entropy Methods: Complexity Analysis of Resting-State fMRI, *IEEE Access* 8 (2020) 124437–124450. [doi:10.1109/ACCESS.2020.3005906](https://doi.org/10.1109/ACCESS.2020.3005906).
- [86] M. K. Gale, M. Nezafati, S. D. Keilholz, Complexity Analysis of Resting-State and Task fMRI Using Multiscale Sample Entropy, in: 2021 43rd Annual International Conference of the IEEE Engineering in Medicine & Biology Society (EMBC), IEEE, Mexico, 2021, pp. 2968–2971. [doi:10.1109/EMBC46164.2021.9630607](https://doi.org/10.1109/EMBC46164.2021.9630607).
- [87] S.-W. Xue, D. Wang, Z. Tan, Y. Wang, Z. Lian, Y. Sun, X. Hu, X. Wang, X. Zhou, Disrupted Brain Entropy And Functional Connectivity Patterns Of Thalamic Subregions In Major Depressive Disorder, *Neuropsychiatric Disease and Treatment* Volume 15 (2019) 2629–2638. [doi:10.2147/NDT.S220743](https://doi.org/10.2147/NDT.S220743).
- [88] G. Del Mauro, L. S. Sevel, J. Boissoneault, Z. Wang, Divergent association between pain intensity and resting-state fMRI -based brain entropy in different age groups, *Journal of Neuroscience Research* 102 (5) (2024) e25341. [doi:10.1002/jnr.25341](https://doi.org/10.1002/jnr.25341).

- [89] G. Del Mauro, X. Zeng, Z. Wang, Normative Brain Entropy Across the Lifespan (May 2025). [doi:10.1101/2025.05.08.652915](https://doi.org/10.1101/2025.05.08.652915).
- [90] G. Del Mauro, Y. Li, J. Yu, P. Kochunov, L. S. Sevel, J. Boissoneault, S. Chen, Z. Wang, Chronic pain is associated with greater brain entropy in the prefrontal cortex, *The Journal of Pain* 32 (2025) 105421. [doi:10.1016/j.jpain.2025.105421](https://doi.org/10.1016/j.jpain.2025.105421).
- [91] R. Zhang, S. Cen, D. Wijesinghe, L. Aksman, S. B. Murray, C. J. Duval, D. J. Wang, K. Jann, Elucidating distinct and common fMRI-complexity patterns in pre-adolescent children with Attention-Deficit/Hyperactivity Disorder, Oppositional Defiant Disorder, and Obsessive-Compulsive Disorder diagnoses (Jan. 2025). [doi:10.1101/2025.01.17.25320748](https://doi.org/10.1101/2025.01.17.25320748).
- [92] M. Nezafati, H. Temmar, S. D. Keilholz, Functional MRI Signal Complexity Analysis Using Sample Entropy, *Frontiers in Neuroscience* 14 (2020) 700. [doi:10.3389/fnins.2020.00700](https://doi.org/10.3389/fnins.2020.00700).
- [93] M. O. Sokunbi, G. G. Cameron, T. S. Ahearn, A. D. Murray, R. T. Staff, Fuzzy approximate entropy analysis of resting state fMRI signal complexity across the adult life span, *Medical Engineering & Physics* 37 (11) (2015) 1082–1090. [doi:10.1016/j.medengphy.2015.09.001](https://doi.org/10.1016/j.medengphy.2015.09.001).
- [94] Z. Li, Z. Fang, N. Hager, H. Rao, Z. Wang, Hyper-resting brain entropy within chronic smokers and its moderation by Sex, *Scientific Reports* 6 (1) (2016) 29435. [doi:10.1038/srep29435](https://doi.org/10.1038/srep29435).
- [95] I.-J. Chi, S.-J. Tsai, C.-H. Chen, A. C. Yang, Identifying Distinct Developmental Patterns of Brain Complexity in Autism: A Cross-Sectional Cohort Analysis Using the Autism Brain Imaging Data Exchange, *Psychiatry and Clinical Neurosciences* 79 (3) (2025) 98–107. [doi:10.1111/pcn.13780](https://doi.org/10.1111/pcn.13780).
- [96] A. Kielar, T. Deschamps, R. K. O. Chu, R. Jokel, Y. B. Khatamian, J. J. Chen, J. A. Meltzer, Identifying Dysfunctional Cortex: Dissociable Effects of Stroke and Aging on Resting State Dynamics in MEG and fMRI, *Frontiers in Aging Neuroscience* 8 (Mar. 2016). [doi:10.3389/fnagi.2016.00040](https://doi.org/10.3389/fnagi.2016.00040).
- [97] H. Liu, W. Gao, W. Cao, Q. Meng, L. Xu, L. Kuang, Y. Guo, D. Cui, J. Qiu, Q. Jiao, L. Su, G. Lu, Immediate visual reproduction negatively correlates with brain entropy of parahippocampal gyrus and inferior occipital gyrus in bipolar II disorder adolescents, *BMC Psychiatry* 23 (1) (2023) 515. [doi:10.1186/s12888-023-05012-3](https://doi.org/10.1186/s12888-023-05012-3).
- [98] N. De Carvalho Santos, G. Gâmbaro, L. L. Da Silva, P. H. R. Da Silva, R. F. Leoni, Impaired brain functional connectivity and complexity in mild cognitive decline, *Brain Organoid and Systems Neuroscience Journal* 3 (2025) 15–24. [doi:10.1016/j.bosn.2025.02.002](https://doi.org/10.1016/j.bosn.2025.02.002).

- [99] D. Song, P. Liu, X. Ma, D. Chang, Z. Wang, Increased resting-state brain entropy (BEN) in mild to moderate depression was decreased by nonpharmacological treatment (Apr. 2024). [doi:10.1101/2024.04.26.24306327](https://doi.org/10.1101/2024.04.26.24306327).
- [100] S.-W. Xue, Y. Guo, Increased resting-state brain entropy in Alzheimer's disease, *NeuroReport* 29 (4) (2018) 286–290. [doi:10.1097/WNR.0000000000000942](https://doi.org/10.1097/WNR.0000000000000942).
- [101] S. Zhang, L. J. Spoletni, B. P. Gold, V. L. Morgan, B. P. Rogers, C. Chang, Interindividual Signatures of fMRI Temporal Fluctuations, *Cerebral Cortex* 31 (10) (2021) 4450–4463. [doi:10.1093/cercor/bhab099](https://doi.org/10.1093/cercor/bhab099).
- [102] J. Festor, Investigating Neuroplasticity in Glioma Patients.
- [103] L. Lin, D. Chang, D. Song, Y. Li, Z. Wang, Lower resting brain entropy is associated with stronger task activation and deactivation, *NeuroImage* 249 (2022) 118875. [doi:10.1016/j.neuroimage.2022.118875](https://doi.org/10.1016/j.neuroimage.2022.118875).
- [104] D. Song, Z. Wang, Neurotransmitters Contribute Structure-Function Coupling: Evidence from Grey Matter Volume (GMV) and Brain Entropy (BEN) (Sep. 2024). [doi:10.1101/2024.09.07.611832](https://doi.org/10.1101/2024.09.07.611832).
- [105] N. Wang, H. Wu, M. Xu, Y. Yang, C. Chang, W. Zeng, H. Yan, Occupational functional plasticity revealed by brain entropy: A resting-state fMRI study of seafarers, *Human Brain Mapping* 39 (7) (2018) 2997–3004. [doi:10.1002/hbm.24055](https://doi.org/10.1002/hbm.24055).
- [106] D. Chang, X. Wang, Y. Chen, Z. R. Han, Y. Wang, B. Liu, Z. Zhang, X.-N. Zuo, Older is order: Entropy reduction in cortical spontaneous activity marks healthy aging, *BMC Neuroscience* 25 (1) (2024) 74. [doi:10.1186/s12868-024-00916-6](https://doi.org/10.1186/s12868-024-00916-6).
- [107] X.-H. Wang, Y. Jiao, L. Li, Predicting clinical symptoms of attention deficit hyperactivity disorder based on temporal patterns between and within intrinsic connectivity networks, *Neuroscience* 362 (2017) 60–69. [doi:10.1016/j.neuroscience.2017.08.038](https://doi.org/10.1016/j.neuroscience.2017.08.038).
- [108] D. Song, D. Chang, J. Zhang, W. Peng, Y. Shang, X. Gao, Z. Wang, Reduced brain entropy by repetitive transcranial magnetic stimulation on the left dorsolateral prefrontal cortex in healthy young adults, *Brain Imaging and Behavior* 13 (2) (2019) 421–429. [doi:10.1007/s11682-018-9866-4](https://doi.org/10.1007/s11682-018-9866-4).
- [109] L. Liang, R. Hu, X. Luo, B. Feng, W. Long, R. Song, Reduced Complexity in Stroke with Motor Deficits: A Resting-State fMRI Study, *Neuroscience* 434 (2020) 35–43. [doi:10.1016/j.neuroscience.2020.03.020](https://doi.org/10.1016/j.neuroscience.2020.03.020).
- [110] D.-H. Song, Z. Wang, Regional Brain Entropy During Movie-watching (Jun. 2024). [doi:10.1101/2024.06.12.598767](https://doi.org/10.1101/2024.06.12.598767).

- [111] J. Lu, D. Song, D. Chang, Z. Wang, Reproducible Brain Entropy (BEN) Alterations During Rumination (Dec. 2024). [doi:10.1101/2024.12.02.626334](https://doi.org/10.1101/2024.12.02.626334).
- [112] F. Zhou, Y. Zhuang, H. Gong, J. Zhan, M. Grossman, Z. Wang, Resting State Brain Entropy Alterations in Relapsing Remitting Multiple Sclerosis, PLOS ONE 11 (1) (2016) e0146080. [doi:10.1371/journal.pone.0146080](https://doi.org/10.1371/journal.pone.0146080).
- [113] M. O. Sokunbi, W. Fung, V. Sawlani, S. Choppin, D. E. Linden, J. Thome, Resting state fMRI entropy probes complexity of brain activity in adults with ADHD, Psychiatry Research: Neuroimaging 214 (3) (2013) 341–348. [doi:10.1016/j.psychresns.2013.10.001](https://doi.org/10.1016/j.psychresns.2013.10.001).
- [114] S.-W. Xue, Q. Yu, Y. Guo, D. Song, Z. Wang, Resting-state brain entropy in schizophrenia, Comprehensive Psychiatry 89 (2019) 16–21. [doi:10.1016/j.comppsych.2018.11.015](https://doi.org/10.1016/j.comppsych.2018.11.015).
- [115] G. D. Mauro, Z. Wang, rsfMRI-based brain entropy is negatively correlated with gray matter volume and surface area, Brain Structure and Function 230 (2) (2025) 35. [doi:10.1007/s00429-025-02897-6](https://doi.org/10.1007/s00429-025-02897-6).
- [116] C.-l. Zhao, W. Hou, Y. Jia, B. J. Sahakian, the DIRECT Consortium, Q. Luo, Sex differences of signal complexity at resting-state functional magnetic resonance imaging and their associations with the estrogen-signaling pathway in the brain, Cognitive Neurodynamics 18 (3) (2024) 973–986. [doi:10.1007/s11571-023-09954-y](https://doi.org/10.1007/s11571-023-09954-y).
- [117] A. Camargo, G. Del Mauro, Z. Wang, Task-induced changes in brain entropy, Journal of Neuroscience Research 102 (2) (2024) e25310. [doi:10.1002/jnr.25310](https://doi.org/10.1002/jnr.25310).
- [118] D. Song, Z. Wang, The relationships of resting-state brain entropy (BEN), ovarian hormones and behavioral inhibition and activation systems (BIS/BAS), NeuroImage 312 (2025) 121226. [doi:10.1016/j.neuroimage.2025.121226](https://doi.org/10.1016/j.neuroimage.2025.121226).
- [119] T. Jordan, M. R. Apostol, J. Nomi, N. Petersen, Unraveling Neural Complexity: Exploring Brain Entropy to Yield Mechanistic Insight in Neuromodulation Therapies for Tobacco Use Disorder (Sep. 2023). [doi:10.1101/2023.09.12.557465](https://doi.org/10.1101/2023.09.12.557465).
- [120] A. Hull, Entropic Voxels Indicate Large Brain-State Repertoires (2022). [arXiv:20.500.14721/25024](https://arxiv.org/abs/20.500.14721/25024).
- [121] D.-H. Song, X.-P. Deng, Y.-Q. Shang, D. Chang, Z. Wang, Altered resting-state brain entropy (BEN) by rTMS across the human cortex (Jul. 2024). [doi:10.1101/2024.07.16.601109](https://doi.org/10.1101/2024.07.16.601109).

- [122] M. O. Sokunbi, V. B. Gradin, G. D. Waiter, G. G. Cameron, T. S. Ahearn, A. D. Murray, D. J. Steele, R. T. Staff, Nonlinear Complexity Analysis of Brain fMRI Signals in Schizophrenia, *PLoS ONE* 9 (5) (2014) e95146. [doi:10.1371/journal.pone.0095146](https://doi.org/10.1371/journal.pone.0095146).
- [123] Q. Li, J. Liu, G. D. Pearlson, J. Chen, Y.-P. Wang, J. A. Turner, V. D. Calhoun, Spatiotemporal Complexity in the Psychotic Brain (Jan. 2025). [doi:10.1101/2025.01.14.632764](https://doi.org/10.1101/2025.01.14.632764).
- [124] P. Liu, D. Song, X. Deng, Y. Shang, Q. Ge, Z. Wang, H. Zhang, The effects of intermittent theta burst stimulation (iTBS) on resting-state brain entropy (BEN), *Neurotherapeutics* 22 (3) (2025) e00556. [doi:10.1016/j.neurot.2025.e00556](https://doi.org/10.1016/j.neurot.2025.e00556).
- [125] E. Stobbe, C. G. Forlim, S. Kühn, Impact of exposure to natural versus urban soundscapes on brain functional connectivity, BOLD entropy and behavior, *Environmental Research* 244 (2024) 117788. [doi:10.1016/j.envres.2023.117788](https://doi.org/10.1016/j.envres.2023.117788).
- [126] F. Zhou, S. Huang, L. Gao, Y. Zhuang, S. Ding, H. Gong, Temporal regularity of intrinsic cerebral activity in patients with chronic primary insomnia: A brain entropy study using resting-state fMRI, *Brain and Behavior* 6 (10) (2016) e00529. [doi:10.1002/brb3.529](https://doi.org/10.1002/brb3.529).
- [127] Q. Li, M. Seraji, V. D. Calhoun, A. Iraji, Complexity Measures of Psychotic Brain Activity in the Fmri Signal (Nov. 2023). [doi:10.1101/2023.11.10.566647](https://doi.org/10.1101/2023.11.10.566647).
- [128] S. Fan, Y. Yu, Y. Wu, Y. Kai, H. Wang, Y. Chen, M. Zu, X. Pang, Y. Tian, Altered brain entropy and functional connectivity patterns in generalized anxiety disorder patients, *Journal of Affective Disorders* 332 (2023) 168–175. [doi:10.1016/j.jad.2023.03.062](https://doi.org/10.1016/j.jad.2023.03.062).
- [129] M. Zhou, W. Jiang, D. Zhong, J. Zheng, Resting-state brain entropy in right temporal lobe epilepsy and its relationship with alertness, *Brain and Behavior* 9 (11) (2019) e01446. [doi:10.1002/brb3.1446](https://doi.org/10.1002/brb3.1446).
- [130] R. Zhang, L. Aksman, D. Wijesinghe, J. M. Ringman, D. J. J. Wang, K. Jann, for the Alzheimer’s Disease Neuroimaging Initiative, A longitudinal study of functional brain complexity in progressive Alzheimer’s disease, *Alzheimer’s & Dementia: Diagnosis, Assessment & Disease Monitoring* 17 (1) (2025) e70059. [doi:10.1002/dad2.70059](https://doi.org/10.1002/dad2.70059).
- [131] S. Guan, D. Wan, R. Zhao, E. Canario, C. Meng, B. B. Biswal, The complexity of spontaneous brain activity changes in schizophrenia, bipolar disorder, and ADHD was examined using different variations of entropy, *Human Brain Mapping* 44 (1) (2023) 94–118. [doi:10.1002/hbm.26129](https://doi.org/10.1002/hbm.26129).

- [132] K. Jann, G. Park, H. Kim, the Alzheimer's Disease Neuroimaging Initiative, Classifying Mild Cognitive Impairment from Normal Cognition: fMRI Complexity Matches Tau PET Performance (Jan. 2025). [doi:10.1101/2025.01.16.633407](https://doi.org/10.1101/2025.01.16.633407).
- [133] D. Su, Y. Cui, Z. Liu, H. Chen, J. Fang, H. Ma, J. Zhou, T. Feng, Altered Brain Activity in Depression of Parkinson's Disease: A Meta-Analysis and Validation Study, *Frontiers in Aging Neuroscience* 14 (2022) 806054. [doi:10.3389/fnagi.2022.806054](https://doi.org/10.3389/fnagi.2022.806054).
- [134] The Alzheimer's Disease Neuroimaging Initiative, P. Ren, M. Ma, G. Xie, Z. Wu, D. Wu, Altered complexity of resting-state BOLD activity in Alzheimer's disease-related neurodegeneration: A multiscale entropy analysis, *Aging* 12 (13) (2020) 13571–13582. [doi:10.18632/aging.103463](https://doi.org/10.18632/aging.103463).
- [135] D. J. Whiteside, P. S. Jones, B. C. P. Ghosh, I. Coyle-Gilchrist, A. Gerhard, M. T. Hu, J. C. Klein, P. N. Leigh, A. Church, D. J. Burn, H. R. Morris, J. B. Rowe, T. Rittman, Altered network stability in progressive supranuclear palsy, *Neurobiology of Aging* 107 (2021) 109–117. [doi:10.1016/j.neurobiolaging.2021.07.007](https://doi.org/10.1016/j.neurobiolaging.2021.07.007).
- [136] M. Peña, K. Petrillo, M. Bosset, M. Fain, Y.-h. Chou, S. Rapcsak, N. Toosizadeh, Brain function complexity during dual-tasking is associated with cognitive impairment and age, *Journal of Neuroimaging* 32 (6) (2022) 1211–1223. [doi:10.1111/jon.13025](https://doi.org/10.1111/jon.13025).
- [137] P.-S. Ho, C. Lin, G.-Y. Chen, H.-L. Liu, C.-M. Huang, T. M.-C. Lee, S.-H. Lee, S.-C. Wu, Complexity analysis of resting state fMRI signals in depressive patients, in: 2017 39th Annual International Conference of the IEEE Engineering in Medicine and Biology Society (EMBC), IEEE, Seogwipo, 2017, pp. 3190–3193. [doi:10.1109/EMBC.2017.8037535](https://doi.org/10.1109/EMBC.2017.8037535).
- [138] A. C. Yang, C.-C. Huang, H.-L. Yeh, M.-E. Liu, C.-J. Hong, P.-C. Tu, J.-F. Chen, N. E. Huang, C.-K. Peng, C.-P. Lin, S.-J. Tsai, Complexity of spontaneous BOLD activity in default mode network is correlated with cognitive function in normal male elderly: A multiscale entropy analysis, *Neurobiology of Aging* 34 (2) (2013) 428–438. [doi:10.1016/j.neurobiolaging.2012.05.004](https://doi.org/10.1016/j.neurobiolaging.2012.05.004).
- [139] G. Trevino, J. J. Lee, J. S. Shimony, P. H. Luckett, E. C. Leuthardt, Complexity organization of resting-state functional- MRI networks, *Human Brain Mapping* 45 (12) (2024) e26809. [doi:10.1002/hbm.26809](https://doi.org/10.1002/hbm.26809).
- [140] Y.-C. Kung, C.-W. Li, F.-C. Hsiao, P.-J. Tsai, S. Chen, M.-K. Li, H.-C. Lee, C.-Y. Chang, C. W. Wu, C.-P. Lin, Cross-Scale Dynamicity of Entropy and Connectivity in the Sleeping Brain, *Brain Connectivity* 12 (9) (2022) 835–845. [doi:10.1089/brain.2021.0174](https://doi.org/10.1089/brain.2021.0174).

- [141] A. C. Yang, C.-J. Hong, Y.-J. Liou, K.-L. Huang, C.-C. Huang, M.-E. Liu, M.-T. Lo, N. E. Huang, C.-K. Peng, C.-P. Lin, S.-J. Tsai, Decreased resting-state brain activity complexity in schizophrenia characterized by both increased regularity and randomness, *Human Brain Mapping* 36 (6) (2015) 2174–2186. [doi:10.1002/hbm.22763](https://doi.org/10.1002/hbm.22763).
- [142] M. Grieder, D. J. J. Wang, T. Dierks, L.-O. Wahlund, K. Jann, Default Mode Network Complexity and Cognitive Decline in Mild Alzheimer's Disease, *Frontiers in Neuroscience* 12 (2018) 770. [doi:10.3389/fnins.2018.00770](https://doi.org/10.3389/fnins.2018.00770).
- [143] Y. Niu, B. Wang, M. Zhou, J. Xue, H. Shapour, R. Cao, X. Cui, J. Wu, J. Xiang, Dynamic Complexity of Spontaneous BOLD Activity in Alzheimer's Disease and Mild Cognitive Impairment Using Multiscale Entropy Analysis, *Frontiers in Neuroscience* 12 (2018) 677. [doi:10.3389/fnins.2018.00677](https://doi.org/10.3389/fnins.2018.00677).
- [144] M. Amalric, J. F. Cantlon, Entropy, complexity, and maturity in children's neural responses to naturalistic video lessons, *Cortex* 163 (2023) 14–25. [doi:10.1016/j.cortex.2023.02.008](https://doi.org/10.1016/j.cortex.2023.02.008).
- [145] I. M. McDonough, S. K. Letang, H. B. Erwin, R. K. Kana, Evidence for Maintained Post-Encoding Memory Consolidation Across the Adult Lifespan Revealed by Network Complexity, *Entropy* 21 (11) (2019) 1072. [doi:10.3390/e21111072](https://doi.org/10.3390/e21111072).
- [146] R. Zhang, S. B. Murray, C. J. Duval, D. J. Wang, K. Jann, Functional connectivity and complexity analyses of resting-state fMRI in pre-adolescents demonstrating the behavioral symptoms of ADHD, *Psychiatry Research* 334 (2024) 115794. [doi:10.1016/j.psychres.2024.115794](https://doi.org/10.1016/j.psychres.2024.115794).
- [147] C. Lin, S.-H. Lee, C.-M. Huang, G.-Y. Chen, P.-S. Ho, H.-L. Liu, Y.-L. Chen, T. M.-C. Lee, S.-C. Wu, Increased brain entropy of resting-state fMRI mediates the relationship between depression severity and mental health-related quality of life in late-life depressed elderly, *Journal of Affective Disorders* 250 (2019) 270–277. [doi:10.1016/j.jad.2019.03.012](https://doi.org/10.1016/j.jad.2019.03.012).
- [148] D. Wijesinghe, K. Lynch, L. Askman, D. C. Delis, D. J. Wang, K. Jann, Lifespan Trajectories of the Brain's Functional Complexity Characterized by Multiscale Sample Entropy (Mar. 2025). [doi:10.1101/2025.03.03.641327](https://doi.org/10.1101/2025.03.03.641327).
- [149] R. X. Smith, L. Yan, D. J. J. Wang, Multiple time scale complexity analysis of resting state FMRI, *Brain Imaging and Behavior* 8 (2) (2014) 284–291. [doi:10.1007/s11682-013-9276-6](https://doi.org/10.1007/s11682-013-9276-6).
- [150] J. Zhou, V. Poole, T. Wooten, O. Lo, I. Illoputaife, M. Esterman, L. Lipsitz, B. Manor, MULTI-SCALE DYNAMICS OF SPONTANOUS BRAIN

ACTIVITY CORRELATE WITH WALKING SPEED IN COMMUNITY-DWELLING OLDER ADULTS, Innovation in Aging 2 (suppl_1) (2018) 365–365. [doi:10.1093/geroni/igy023.1348](https://doi.org/10.1093/geroni/igy023.1348).

- [151] G. Yuan, Y. Zheng, Y. Wang, X. Qi, R. Wang, Z. Ma, X. Guo, X. Wang, J. Zhang, Multiscale entropy and small-world network analysis in rs-fMRI — new tools to evaluate early basal ganglia dysfunction in diabetic peripheral neuropathy, *Frontiers in Endocrinology* 13 (2022) 974254. [doi:10.3389/fendo.2022.974254](https://doi.org/10.3389/fendo.2022.974254).
- [152] K. Kadota, K. Onoda, S. Abe, C. Hamada, S. Mitaki, H. Oguro, A. Nagai, H. Kitagaki, S. Yamaguchi, Multiscale Entropy of Resting-State Functional Magnetic Resonance Imaging Differentiates Progressive Supranuclear Palsy and Multiple System Atrophy, *Life* 11 (12) (2021) 1411. [doi:10.3390/life11121411](https://doi.org/10.3390/life11121411).
- [153] D. E.-W. McCulloch, A. S. Olsen, B. Ozenne, D. S. Stenbaek, S. Armand, M. K. Madsen, G. M. Knudsen, P. M. Fisher, Navigating the chaos of psychedelic fMRI brain-entropy via multi-metric evaluations of acute psilocybin effects (Jul. 2023). [doi:10.1101/2023.07.03.23292164](https://doi.org/10.1101/2023.07.03.23292164).
- [154] I. M. McDonough, K. Nashiro, Network complexity as a measure of information processing across resting-state networks: Evidence from the Human Connectome Project, *Frontiers in Human Neuroscience* 8 (Jun. 2014). [doi:10.3389/fnhum.2014.00409](https://doi.org/10.3389/fnhum.2014.00409).
- [155] B. Hager, A. C. Yang, R. Brady, S. Meda, B. Clementz, G. D. Pearlson, J. A. Sweeney, C. Tamminga, M. Keshavan, Neural complexity as a potential translational biomarker for psychosis, *Journal of Affective Disorders* 216 (2017) 89–99. [doi:10.1016/j.jad.2016.10.016](https://doi.org/10.1016/j.jad.2016.10.016).
- [156] D. J. J. Wang, K. Jann, C. Fan, Y. Qiao, Y.-F. Zang, H. Lu, Y. Yang, Neurophysiological Basis of Multi-Scale Entropy of Brain Complexity and Its Relationship With Functional Connectivity, *Frontiers in Neuroscience* 12 (2018) 352. [doi:10.3389/fnins.2018.00352](https://doi.org/10.3389/fnins.2018.00352).
- [157] F. Yang, F. Zhang, A. N. Belkacem, C. Xie, Y. Wang, S. Chen, Z. Yang, Z. Song, M. Ge, C. Chen, Optimized Multiscale Entropy Model Based on Resting-State fMRI for Appraising Cognitive Performance in Healthy Elderly, *Computational and Mathematical Methods in Medicine* 2022 (2022) 1–12. [doi:10.1155/2022/2484081](https://doi.org/10.1155/2022/2484081).
- [158] H. Zheng, K. Onoda, A. Nagai, S. Yamaguchi, Reduced Dynamic Complexity of BOLD Signals Differentiates Mild Cognitive Impairment From Normal Aging, *Frontiers in Aging Neuroscience* 12 (2020) 90. [doi:10.3389/fnagi.2020.00090](https://doi.org/10.3389/fnagi.2020.00090).
- [159] X. Wang, Y. Zhang, S. Han, J. Zhao, H. Chen, Resting-State Brain Activity Complexity in Early-Onset Schizophrenia Characterized by a Multi-scale Entropy Method, in: Y. Sun, H. Lu, L. Zhang, J. Yang, H. Huang

(Eds.), Intelligence Science and Big Data Engineering, Vol. 10559, Springer International Publishing, Cham, 2017, pp. 580–588. [doi:10.1007/978-3-319-67777-4_52](https://doi.org/10.1007/978-3-319-67777-4_52).

- [160] A. Omidvarnia, A. Zalesky, S. Mansour L, D. Van De Ville, G. D. Jackson, M. Pedersen, Temporal complexity of fMRI is reproducible and correlates with higher order cognition, *NeuroImage* 230 (2021) 117760. [doi:10.1016/j.neuroimage.2021.117760](https://doi.org/10.1016/j.neuroimage.2021.117760).
- [161] A. C. Yang, C.-C. Huang, M.-E. Liu, Y.-J. Liou, C.-J. Hong, M.-T. Lo, N. E. Huang, C.-K. Peng, C.-P. Lin, S.-J. Tsai, The APOE 4 allele affects complexity and functional connectivity of resting brain activity in healthy adults: APOE and Resting Brain Complexity, *Human Brain Mapping* 35 (7) (2014) 3238–3248. [doi:10.1002/hbm.22398](https://doi.org/10.1002/hbm.22398).
- [162] Y. Zhen, Y. Yang, Y. Zheng, X. Wang, L. Liu, Z. Zheng, H. Zheng, S. Tang, The heritability and structural correlates of resting-state fMRI complexity, *NeuroImage* 296 (2024) 120657. [doi:10.1016/j.neuroimage.2024.120657](https://doi.org/10.1016/j.neuroimage.2024.120657).
- [163] W. Xiao, M. Jones, Multiscale Entropy of Resting-State fMRI Signals Reveals Differences in Brain Complexity in Autism (May 2025). [doi:10.1101/2025.05.22.655518](https://doi.org/10.1101/2025.05.22.655518).
- [164] I. M. McDonough, J. T. Siegel, The Relation Between White Matter Microstructure and Network Complexity: Implications for Processing Efficiency, *Frontiers in Integrative Neuroscience* 12 (2018) 43. [doi:10.3389/fnint.2018.00043](https://doi.org/10.3389/fnint.2018.00043).
- [165] A. Omidvarnia, L. Sasse, D. I. Larabi, F. Raimondo, F. Hoffstaedter, J. Kasper, J. Dukart, M. Petersen, B. Cheng, G. Thomalla, S. B. Eickhoff, K. R. Patil, Is resting state fMRI better than individual characteristics at predicting cognition? (Feb. 2023). [doi:10.1101/2023.02.18.529076](https://doi.org/10.1101/2023.02.18.529076).
- [166] A. Omidvarnia, R. Liégeois, E. Amico, M. G. Preti, A. Zalesky, D. Van De Ville, On the Spatial Distribution of Temporal Complexity in Resting State and Task Functional MRI, *Entropy* 24 (8) (2022) 1148. [doi:10.3390/e24081148](https://doi.org/10.3390/e24081148).
- [167] R. X. Smith, K. Jann, B. Ances, D. J. Wang, Wavelet-based regularity analysis reveals recurrent spatiotemporal behavior in resting-state fMRI, *Human Brain Mapping* 36 (9) (2015) 3603–3620. [doi:10.1002/hbm.22865](https://doi.org/10.1002/hbm.22865).
- [168] L. Xu, J. Feng, L. Yu, Avalanche criticality in individuals, fluid intelligence, and working memory, *Human Brain Mapping* 43 (8) (2022) 2534–2553. [doi:10.1002/hbm.25802](https://doi.org/10.1002/hbm.25802).

- [169] O. Campbell, T. Vanderwal, A. M. Weber, Fractal-Based Analysis of fMRI BOLD Signal During Naturalistic Viewing Conditions, *Frontiers in Physiology* 12 (2022) 809943. [doi:10.3389/fphys.2021.809943](https://doi.org/10.3389/fphys.2021.809943).
- [170] A. E. Mella, T. Vanderwal, S. P. Miller, A. M. Weber, Temporal complexity of the BOLD-signal in preterm versus term infants, *Cerebral Cortex* 34 (10) (2024) bhae426. [doi:10.1093/cercor/bhae426](https://doi.org/10.1093/cercor/bhae426).
- [171] J. M. Beggs, *The Cortex and the Critical Point*, 1st Edition, MIT Press Direct, Cambridge, MA, 2022.
- [172] G. Buzsáki, *Rhythms of the Brain*, Oxford University Press, 2006. [doi:10.1093/acprof:oso/9780195301069.001.0001](https://doi.org/10.1093/acprof:oso/9780195301069.001.0001).
- [173] R. T. Canolty, R. T. Knight, The functional role of cross-frequency coupling, *Trends in Cognitive Sciences* 14 (11) (2010) 506–515. [doi:10.1016/j.tics.2010.09.001](https://doi.org/10.1016/j.tics.2010.09.001).
- [174] G. Werner, Fractals in the nervous system: Conceptual implications for theoretical neuroscience, *Frontiers in Physiology* (2010). [doi:10.3389/fphys.2010.00015](https://doi.org/10.3389/fphys.2010.00015).
- [175] M. Costa, J. Healey, Multiscale entropy analysis of complex heart rate dynamics: Discrimination of age and heart failure effects, in: *Computers in Cardiology, 2003, IEEE, Thessaloniki Chalkidiki, Greece, 2003*, pp. 705–708. [doi:10.1109/CIC.2003.1291253](https://doi.org/10.1109/CIC.2003.1291253).
- [176] J. Q. Kosciessa, N. A. Kloosterman, D. D. Garrett, Standard multiscale entropy reflects neural dynamics at mismatched temporal scales: What's signal irregularity got to do with it?, *PLOS Computational Biology* 16 (5) (2020) e1007885. [doi:10.1371/journal.pcbi.1007885](https://doi.org/10.1371/journal.pcbi.1007885).
- [177] Y. Niu, J. Sun, B. Wang, Y. Yang, X. Wen, J. Xiang, Trajectories of brain entropy across lifetime estimated by resting state functional magnetic resonance imaging, *Human Brain Mapping* 43 (14) (2022) 4359–4369. [doi:10.1002/hbm.25959](https://doi.org/10.1002/hbm.25959).
- [178] B. Wang, Y. Niu, L. Miao, R. Cao, P. Yan, H. Guo, D. Li, Y. Guo, T. Yan, J. Wu, J. Xiang, H. Zhang, Decreased Complexity in Alzheimer's Disease: Resting-State fMRI Evidence of Brain Entropy Mapping, *Frontiers in Aging Neuroscience* 9 (2017) 378. [doi:10.3389/fnagi.2017.00378](https://doi.org/10.3389/fnagi.2017.00378).
- [179] S. Ji, F. Chen, S. Li, C. Zhou, C. Liu, H. Yu, Dynamic brain entropy predicts risky decision-making across transdiagnostic dimensions of psychopathology, *Behavioural Brain Research* 476 (2025) 115255. [doi:10.1016/j.bbr.2024.115255](https://doi.org/10.1016/j.bbr.2024.115255).

- [180] A. Wohlschläger, H. Karne, D. Jordan, M. J. Lowe, S. E. Jones, A. Anand, Spectral Dynamics of Resting State fMRI Within the Ventral Tegmental Area and Dorsal Raphe Nuclei in Medication-Free Major Depressive Disorder in Young Adults, *Frontiers in Psychiatry* 9 (2018) 163. [doi:10.3389/fpsyg.2018.00163](https://doi.org/10.3389/fpsyg.2018.00163).
- [181] L. Liu, Z. Li, D. Kong, Y. Huang, D. Wu, H. Zhao, X. Gao, X. Zhang, M. Yang, Neuroimaging markers of aberrant brain activity and treatment response in schizophrenia patients based on brain complexity, *Translational Psychiatry* 14 (1) (2024) 365. [doi:10.1038/s41398-024-03067-8](https://doi.org/10.1038/s41398-024-03067-8).
- [182] J. Xiang, Y. Tan, Y. Niu, J. Sun, N. Zhang, D. Li, B. Wang, Analysis of functional MRI signal complexity based on permutation fuzzy entropy in bipolar disorder, *NeuroReport* 32 (6) (2021) 465–471. [doi:10.1097/WNR.0000000000001617](https://doi.org/10.1097/WNR.0000000000001617).
- [183] H. A. Velioglu, S. Yıldız, E. Ozdemir-Oktem, S. Cankaya, A. K. Lundmark, A. Ozsimsek, L. Hanoglu, B. Yulug, Smoking affects global and regional brain entropy in depression patients regardless of depression: Preliminary findings, *Journal of Psychiatric Research* 177 (2024) 147–152. [doi:10.1016/j.jpsychires.2024.07.002](https://doi.org/10.1016/j.jpsychires.2024.07.002).
- [184] M. Golesorkhi, J. Gomez-Pilar, Y. Çatal, S. Tumati, M. C. E. Yagoub, E. A. Stamatakis, G. Northoff, From temporal to spatial topography: Hierarchy of neural dynamics in higher- and lower-order networks shapes their complexity, *Cerebral Cortex* 32 (24) (2022) 5637–5653. [doi:10.1093/cercor/bhac042](https://doi.org/10.1093/cercor/bhac042).
- [185] P. A. M. Mediano, A. Ikkala, R. A. Kievit, S. R. Jagannathan, T. F. Varley, E. A. Stamatakis, T. A. Bekinschtein, D. Bor, Fluctuations in Neural Complexity During Wakefulness Relate To Conscious Level and Cognition (Sep. 2021). [doi:10.1101/2021.09.23.461002](https://doi.org/10.1101/2021.09.23.461002).
- [186] C. Bandt, B. Pompe, Permutation Entropy: A Natural Complexity Measure for Time Series, *Physical Review Letters* 88 (17) (2002) 174102. [doi:10.1103/PhysRevLett.88.174102](https://doi.org/10.1103/PhysRevLett.88.174102).
- [187] M. Zanin, L. Zunino, O. A. Rosso, D. Papo, Permutation Entropy and Its Main Biomedical and Econophysics Applications: A Review, *Entropy* 14 (8) (2012) 1553–1577. [doi:10.3390/e14081553](https://doi.org/10.3390/e14081553).
- [188] B. Fadlallah, B. Chen, A. Keil, J. Príncipe, Weighted-permutation entropy: A complexity measure for time series incorporating amplitude information, *Physical Review E* 87 (2) (2013) 022911. [doi:10.1103/PhysRevE.87.022911](https://doi.org/10.1103/PhysRevE.87.022911).
- [189] A. Omidvarnia, M. Mesbah, M. Pedersen, G. Jackson, Range Entropy: A Bridge between Signal Complexity and Self-Similarity, *Entropy* 20 (12) (2018) 962. [doi:10.3390/e20120962](https://doi.org/10.3390/e20120962).

- [190] M. Rostaghi, H. Azami, Dispersion Entropy: A Measure for Time-Series Analysis, *IEEE Signal Processing Letters* 23 (5) (2016) 610–614. [doi:10.1109/LSP.2016.2542881](https://doi.org/10.1109/LSP.2016.2542881).
- [191] T. M. Cover, J. A. Thomas, *Elements of Information Theory*, 1st Edition, Wiley, 2005. [doi:10.1002/047174882X](https://doi.org/10.1002/047174882X).
- [192] R.-N. Duan, J.-Y. Zhu, B.-L. Lu, Differential entropy feature for EEG-based emotion classification, in: 2013 6th International IEEE/EMBS Conference on Neural Engineering (NER), IEEE, San Diego, CA, USA, 2013, pp. 81–84. [doi:10.1109/NER.2013.6695876](https://doi.org/10.1109/NER.2013.6695876).
- [193] R. Taylor, Personal reflections on Jackson Pollock's fractal paintings, *História, Ciências, Saúde-Manguinhos* 13 (suppl) (2006) 109–123. [doi:10.1590/S0104-59702006000500007](https://doi.org/10.1590/S0104-59702006000500007).
- [194] A. Eke, P. Hermán, J. Bassingthwaigte, G. Raymond, D. Percival, M. Cannon, I. Balla, C. Ikrényi, Physiological time series: Distinguishing fractal noises from motions, *Pflügers Archiv - European Journal of Physiology* 439 (4) (2000) 403–415. [doi:10.1007/s004249900135](https://doi.org/10.1007/s004249900135).
- [195] A. Akhrif, M. Romanos, K. Domschke, A. Schmitt-Boehrer, S. Neufang, Fractal Analysis of BOLD Time Series in a Network Associated With Waiting Impulsivity, *Frontiers in Physiology* 9 (2018) 1378. [doi:10.3389/fphys.2018.01378](https://doi.org/10.3389/fphys.2018.01378).
- [196] A. Barnes, E. T. Bullmore, J. Suckling, Endogenous Human Brain Dynamics Recover Slowly Following Cognitive Effort, *PLoS ONE* 4 (8) (2009) e6626. [doi:10.1371/journal.pone.0006626](https://doi.org/10.1371/journal.pone.0006626).
- [197] N. W. Churchill, B. Cimprich, M. K. Askren, P. A. Reuter-Lorenz, M. S. Jung, S. Peltier, M. G. Berman, Scale-free brain dynamics under physical and psychological distress: Pre-treatment effects in women diagnosed with breast cancer, *Human Brain Mapping* 36 (3) (2015) 1077–1092. [doi:10.1002/hbm.22687](https://doi.org/10.1002/hbm.22687).
- [198] N. W. Churchill, R. Spring, C. Grady, B. Cimprich, M. K. Askren, P. A. Reuter-Lorenz, M. S. Jung, S. Peltier, S. C. Strother, M. G. Berman, The suppression of scale-free fMRI brain dynamics across three different sources of effort: Aging, task novelty and task difficulty, *Scientific Reports* 6 (1) (2016) 30895. [doi:10.1038/srep30895](https://doi.org/10.1038/srep30895).
- [199] P. Ciuciu, P. Abry, B. J. He, Interplay between functional connectivity and scale-free dynamics in intrinsic fMRI networks, *NeuroImage* 95 (2014) 248–263. [doi:10.1016/j.neuroimage.2014.03.047](https://doi.org/10.1016/j.neuroimage.2014.03.047).
- [200] O. Dona, G. B. Hall, M. D. Noseworthy, Temporal fractal analysis of the rs-BOLD signal identifies brain abnormalities in autism spectrum disorder, *PLOS ONE* 12 (12) (2017) e0190081. [doi:10.1371/journal.pone.0190081](https://doi.org/10.1371/journal.pone.0190081).

- [201] O. Dona, M. D. Noseworthy, C. DeMatteo, J. F. Connolly, Fractal Analysis of Brain Blood Oxygenation Level Dependent (BOLD) Signals from Children with Mild Traumatic Brain Injury (mTBI), PLOS ONE 12 (1) (2017) e0169647. [doi:10.1371/journal.pone.0169647](https://doi.org/10.1371/journal.pone.0169647).
- [202] J. Dong, B. Jing, X. Ma, H. Liu, X. Mo, H. Li, Hurst Exponent Analysis of Resting-State fMRI Signal Complexity across the Adult Lifespan, Frontiers in Neuroscience 12 (2018) 34. [doi:10.3389/fnins.2018.00034](https://doi.org/10.3389/fnins.2018.00034).
- [203] J. P. Drayne, A. E. Mella, M. M. McLean, S. Ufkes, V. Chau, T. Guo, H. M. Branson, E. Kelly, S. P. Miller, R. E. Grunau, A. M. Weber, Long-range temporal correlation development in resting-state fMRI signal in preterm infants: Scanned shortly after birth and at term-equivalent age, PLOS Complex Systems 1 (4) (2024) e0000024. [doi:10.1371/journal.pcsy.0000024](https://doi.org/10.1371/journal.pcsy.0000024).
- [204] N. Erbil, G. Deshpande, Scale-Free Dynamics of Resting-State fMRI Microstates, Fractal and Fractional 9 (2) (2025) 112. [doi:10.3390/fractfract9020112](https://doi.org/10.3390/fractfract9020112).
- [205] W. Gao, S. Chen, B. Biswal, X. Lei, J. Yuan, Temporal dynamics of spontaneous default-mode network activity mediate the association between reappraisal and depression, Social Cognitive and Affective Neuroscience (Oct. 2018). [doi:10.1093/scan/nsy092](https://doi.org/10.1093/scan/nsy092).
- [206] W. Gao, B. Biswal, J. Yang, S. Li, Y. Wang, S. Chen, J. Yuan, Temporal dynamic patterns of the ventromedial prefrontal cortex underlie the association between rumination and depression, Cerebral Cortex 33 (4) (2023) 969–982. [doi:10.1093/cercor/bhac115](https://doi.org/10.1093/cercor/bhac115).
- [207] C. Gentili, I. A. Cristea, E. Ricciardi, N. Vanello, C. Popita, D. David, P. Pietrini, Not in one metric: Neuroticism modulates different resting state metrics within distinctive brain regions, Behavioural Brain Research 327 (2017) 34–43. [doi:10.1016/j.bbr.2017.03.031](https://doi.org/10.1016/j.bbr.2017.03.031).
- [208] C. Gentili, N. Vanello, I. Cristea, D. David, E. Ricciardi, P. Pietrini, Proneness to social anxiety modulates neural complexity in the absence of exposure: A resting state fMRI study using Hurst exponent, Psychiatry Research: Neuroimaging 232 (2) (2015) 135–144. [doi:10.1016/j.psychresns.2015.03.005](https://doi.org/10.1016/j.psychresns.2015.03.005).
- [209] A.-T. P. Jäger, A. Bailey, J. M. Huntenburg, C. L. Tardif, A. Villringer, C. J. Gauthier, V. Nikulin, P.-L. Bazin, C. J. Steele, Decreased long-range temporal correlations in the RESTING-STATE FUNCTIONAL MAGNETIC RESONANCE IMAGING BLOOD-OXYGEN-LEVEL-DEPENDENT signal reflect motor sequence learning up to 2 weeks following training, Human Brain Mapping 45 (4) (2024) e26539. [doi:10.1002/hbm.26539](https://doi.org/10.1002/hbm.26539).

- [210] M.-C. Lai, M. V. Lombardo, B. Chakrabarti, S. A. Sadek, G. Pasco, S. J. Wheelwright, E. T. Bullmore, S. Baron-Cohen, J. Suckling, A Shift to Randomness of Brain Oscillations in People with Autism, *Biological Psychiatry* 68 (12) (2010) 1092–1099. [doi:10.1016/j.biopsych.2010.06.027](https://doi.org/10.1016/j.biopsych.2010.06.027).
- [211] X. Lei, Z. Zhao, H. Chen, Extraversion is encoded by scale-free dynamics of default mode network, *NeuroImage* 74 (2013) 52–57. [doi:10.1016/j.neuroimage.2013.02.020](https://doi.org/10.1016/j.neuroimage.2013.02.020).
- [212] Y. Lei, Y. Li, L. Yu, L. Xu, X. Zhang, G. Zheng, L. Chen, W. Zhang, X. Qi, Y. Gu, Y. Yu, Y. Mao, Faded Critical Dynamics in Adult Moyamoya Disease Revealed by EEG and fMRI, *Oxidative Medicine and Cellular Longevity* 2021 (1) (2021) 6640108. [doi:10.1155/2021/6640108](https://doi.org/10.1155/2021/6640108).
- [213] A. C. Linke, B. Chen, L. Olson, M. Cordova, M. Wilkinson, T. Wang, M. Herrera, M. Salmina, A. Rios, J. Mahmalji, T. Do, J. Vu, M. Budman, A. Walker, I. Fishman, Altered Development of the Hurst Exponent in the Medial Prefrontal Cortex in Preschoolers With Autism, *Biological Psychiatry: Cognitive Neuroscience and Neuroimaging* (2024) S2451902224002714 [doi:10.1016/j.bpsc.2024.09.003](https://doi.org/10.1016/j.bpsc.2024.09.003).
- [214] V. Maxim, L. Şendur, J. Fadili, J. Suckling, R. Gould, R. Howard, E. Bullmore, Fractional Gaussian noise, functional MRI and Alzheimer's disease, *NeuroImage* 25 (1) (2005) 141–158. [doi:10.1016/j.neuroimage.2004.10.044](https://doi.org/10.1016/j.neuroimage.2004.10.044).
- [215] A. Omidvarnia, R. Liégeois, E. Amico, M. G. Preti, A. Zalesky, D. Van De Ville, Assessment of temporal complexity in functional MRI between rest and task conditions (Nov. 2021). [doi:10.1101/2021.11.20.469367](https://doi.org/10.1101/2021.11.20.469367).
- [216] D. Rubin, T. Fekete, L. R. Mujica-Parodi, Optimizing Complexity Measures for fMRI Data: Algorithm, Artifact, and Sensitivity, *PLoS ONE* 8 (5) (2013) e63448. [doi:10.1371/journal.pone.0063448](https://doi.org/10.1371/journal.pone.0063448).
- [217] J. Suckling, A. M. Wink, F. A. Bernard, A. Barnes, E. Bullmore, Endogenous multifractal brain dynamics are modulated by age, cholinergic blockade and cognitive performance, *Journal of Neuroscience Methods* 174 (2) (2008) 292–300. [doi:10.1016/j.jneumeth.2008.06.037](https://doi.org/10.1016/j.jneumeth.2008.06.037).
- [218] A. M. Wink, F. Bernard, R. Salvador, E. Bullmore, J. Suckling, Age and cholinergic effects on hemodynamics and functional coherence of human hippocampus, *Neurobiology of Aging* 27 (10) (2006) 1395–1404. [doi:10.1016/j.neurobiolaging.2005.08.011](https://doi.org/10.1016/j.neurobiolaging.2005.08.011).
- [219] A. Tetereva, S. Kartashov, A. Ivanitsky, O. Martynova, Variance and Scale-Free Properties of Resting-State Blood Oxygenation Level-Dependent Signal After Fear Memory Acquisition and Extinction, *Frontiers in Human Neuroscience* 14 (2020) 509075. [doi:10.3389/fnhum.2020.509075](https://doi.org/10.3389/fnhum.2020.509075).

- [220] L. C. Uscătescu, C. J. Hyatt, J. Dunn, M. Kronbichler, V. Calhoun, S. Corbera, K. Pelphrey, B. Pittman, G. Pearlson, M. Assaf, Using the Excitation/Inhibition Ratio to Optimize the Classification of Autism and Schizophrenia (May 2022). [doi:10.1101/2022.05.24.22275531](https://doi.org/10.1101/2022.05.24.22275531).
- [221] T. F. Varley, M. Craig, R. Adapa, P. Finoia, G. Williams, J. Allanson, J. Pickard, D. K. Menon, E. A. Stamatakis, Fractal dimension of cortical functional connectivity networks & severity of disorders of consciousness, *PLOS ONE* 15 (2) (2020) e0223812. [doi:10.1371/journal.pone.0223812](https://doi.org/10.1371/journal.pone.0223812).
- [222] M. A. Warsi, W. Molloy, M. D. Noseworthy, Correlating brain blood oxygenation level dependent (BOLD) fractal dimension mapping with magnetic resonance spectroscopy (MRS) in Alzheimer's disease, *Magnetic Resonance Materials in Physics, Biology and Medicine* 25 (5) (2012) 335–344. [doi:10.1007/s10334-012-0312-0](https://doi.org/10.1007/s10334-012-0312-0).
- [223] A. M. Weber, N. Soreni, M. D. Noseworthy, A preliminary study on the effects of acute ethanol ingestion on default mode network and temporal fractal properties of the brain, *Magnetic Resonance Materials in Physics, Biology and Medicine* 27 (4) (2014) 291–301. [doi:10.1007/s10334-013-0420-5](https://doi.org/10.1007/s10334-013-0420-5).
- [224] A.-M. Wink, E. Bullmore, A. Barnes, F. Bernard, J. Suckling, Monofractal and multifractal dynamics of low frequency endogenous brain oscillations in functional MRI, *Human Brain Mapping* 29 (7) (2008) 791–801. [doi:10.1002/hbm.20593](https://doi.org/10.1002/hbm.20593).
- [225] K. Xie, J. Royer, R. Rodriguez-Cruces, L. Horwood, A. Ngo, T. Arafat, H. Auer, E. Sahlas, J. Chen, Y. Zhou, S. L. Valk, S.-J. Hong, B. Frauscher, R. Pana, A. Bernasconi, N. Bernasconi, L. Concha, B. Bernhardt, Pharmaco-resistant temporal lobe epilepsy gradually perturbs the cortex-wide excitation-inhibition balance (Apr. 2024). [doi:10.1101/2024.04.22.590555](https://doi.org/10.1101/2024.04.22.590555).